UNIVERSAL
LIBRARY

G. B. BENEDEK

Magnetic Resonance at High Pressure

INTERSCIENCE TRACTS ON PHYSICS AND ASTRONOMY

Edited by R. E. Marshak
University of Rochester

1. **D. J. Hughes**
   NEUTRON OPTICS
2. **M. S. Livingston**
   HIGH-ENERGY ACCELERATORS
3. **L. Spitzer, Jr.**
   PHYSICS OF FULLY IONIZED GASES
   second edition
4. **T. G. Cowling**
   MAGNETOHYDRODYNAMICS
5. **D. ter Haar**
   INTRODUCTION TO THE PHYSICS OF MANY-BODY SYSTEMS
6. **E. J. Öpik**
   PHYSICS OF METEOR FLIGHT IN THE ATMOSPHERE
7. **K. Mendelssohn**
   CRYOPHYSICS
8. **J. L. Delcroix**
   INTRODUCTION TO THE THEORY OF IONIZED GASES
9. **T. E. Sterne**
   AN INTRODUCTION TO CELESTIAL MECHANICS
10. **J. Weber**
    GENERAL RELATIVITY AND GRAVITATIONAL WAVES
11. **R. E. Marshak and E. C. G. Sudarshan**
    INTRODUCTION TO ELEMENTARY PARTICLE PHYSICS
12. **J. L. Olsen**
    ELECTRON TRANSPORT IN METALS
13. **M. Françon**
    MODERN APPLICATIONS OF PHYSICAL OPTICS

14. **P. B. Jones**
THE OPTICAL MODEL IN NUCLEAR AND PARTICLE PHYSICS

15. **R. K. Adair and E. C. Fowler**
STRANGE PARTICLES

16. **R. Wilson**
THE NUCLEON-NUCLEON INTERACTION: EXPERIMENTAL AND PHENOMENOLOGICAL ASPECTS

17. **J. F. Denisse and J. L. Decroix**
PLASMA WAVES

18. **W. F. Brown, Jr.**
MICROMAGNETICS

19. **A. Rose**
CONCEPTS IN PHOTOCONDUCTIVITY AND ALLIED PROBLEMS

20. **A. Guinier and D. L. Dexter**
X-RAY STUDIES OF MATERIALS

21. **T. G. Northrup**
THE ADIABATIC MOTION OF CHARGED PARTICLES

22. **G. Barton**
INTRODUCTION TO ADVANCED FIELD THEORY

23. **C. D. Jeffries**
DYNAMIC NUCLEAR ORIENTATION

24. **G. B. Benedek**
MAGNETIC RESONANCE AT HIGH PRESSURE

Additional volumes in preparation

MAGNETIC RESONANCE AT HIGH PRESSURE

G. B. BENEDEK

Massachusetts Institute of Technology

Cambridge, Massachusetts

1963

INTERSCIENCE PUBLISHERS

a division of John Wiley & Sons,
New York • London

Library of Congress Catalog Card Number 63-18561
Printed in the United States of America by
Mack Printing Co., Easton, Pa.

Preface

The lattice parameter, or the density, stands on an equal footing with the temperature in the theoretical description of a solid, liquid, or gas. This close connection with the theory is the basis for the importance of experiments conducted under high pressure. As the ingenious and prolific work of P. W. Bridgman has demonstrated, a very wide class of experiments can in fact be performed under conditions of high pressure. In 1953, a new class of experiments was added when the author and E. M. Purcell showed that it was possible to perform nuclear resonance experiments to 10,000 bars. Later developments by W. M. Walsh and N. Bloembergen extended the frequency range into the microwave region. Very recently the author and J. D. Litster have shown that it is possible to carry out nuclear resonance experiments into the pressure region above 50,000 bars. Today the experimenter can perform microwave and radiofrequency magnetic resonance experiments which enable him to examine the microscopic details of electronic structure and atomic or molecular motion, while at the same time he varies both the fundamental parameters—the pressure and the temperature—over the range 1 bar $\leq P \leq 10^5$ bar, and $1.5°\text{K} \leq T \leq 400°\text{K}$.

This tract presents an account of experiments performed in this field in sufficient detail so that the reader can see both the power and the limitations of the method. In so doing we cover a wide range of physical phenomena: from the magnetic properties of ferromagnetic metals to the self diffusion of molecules in liquids and gases. In each case the presentation has focused on the physical principles involved and the new information obtained by experiment. Generous literature references have been

provided to enable the reader to obtain further theoretical and experimental details from the original work. As an aid to the experimenter I have included in a short Appendix an account of some of the principal techniques that are used in magnetic resonance experiments at high pressure. In addition to an examination of the present state of the field, the author has endeavored both by organization of the material and by direct suggestion to point out still fruitful areas for experimentation.

While the present material is devoted to magnetic resonance at high pressure, it is important to recognize that were we to extend our attention beyond the radio frequency and microwave region we would find that optical spectroscopy of solids may be carried out to 100,000 bars, as the work of H. Drickamer has shown. Beyond the optical region, x-ray diffraction and γ-ray spectroscopy has been used successfully to study the properties of solids at high pressure. For example, we include in this tract a discussion of the effect of pressure on the energy of the 14.4-kev γ-ray emitted by the Fe^{57} nucleus in ferromagnetic iron. Today experiments on the properties of matter under high pressure have been conducted using electromagnetic radiation whose frequency ranges all the way from d. c. to 10^{18} cps.

In addition to this great breadth available in the electromagnetic spectrum, the stress applied to the sample need not be confined solely to hydrostatic pressure. Important magnetic resonance experiments have been conducted by G. Feher, G. Watkins, R. G. Shulman, and others on solids subjected to uniaxial stress. However, in this short tract it will not be possible to include an account of their work.

In the interests of clarity we include a note on the units most frequently employed in high pressure work—the kilogram per cm^2, the atmosphere, and the bar. These have the following relations to one another and to other commonly used units: 1 kg/cm^2 = 0.9678 atm = 0.9807 bar = 14.22 pounds/inch = 0.9807 $\times$ 10^6 dynes/cm^2.

Finally, I should like to express my thanks to Dr. W. M. Walsh, Jr., for a careful reading of the manuscript and a number of helpful suggestions. I am also grateful to the John S. Guggenheim Foundation for the grant of a fellowship during the term of which this tract was begun.

G. B. BENEDEK

Massachusetts Institute of Technology

Contents

Chapter I

Solids at High Pressure

1. Magnetic Fields in Solids

1.1 Introduction

Both nuclei with magnetic moments and unpaired electrons serve as sensitive probes of the magnetic fields in a solid, and both have been used to study these internal fields.

In the nuclear case, a magnetic field H at the position of a nucleus interacts with the nuclear magnetic moment $g_N\beta_N\mathbf{I}$ to produce a set of energy levels

$$E(m) = -g_N\beta_N H m_I \tag{1-1}$$

where m_I is the magnetic quantum number corresponding to the nuclear spin $\mathbf{I}$, and g_N and β_N are respectively the nuclear g value, and the nuclear magneton (1) $\beta_N = e\hbar/2MC$. By applying to the nuclear moments a perturbing radio-frequency field perpendicular to H, resonant absorption of rf power may be observed when the frequency of the perturbing field corresponds to splittings for which $\Delta m_I = \pm 1$. Measurement of the resonance frequency ν thus enables determination of the field H by the relation

$$\nu = (g_N\beta_N/h)H \tag{1-2}$$

In favorable cases the line width ($\Delta\nu$) of the nuclear absorption is very small compared to the resonance frequency, and hence a very accurate determination of H is possible.

Apart from an externally applied field, the magnetic field at a nucleus is produced by both the orbital and the spin magnetic

moments of the surrounding electrons. In solids the crystalline electric fields frequently quench the orbital angular momentum so that in first approximation we may confine our attention to the effects of the spin magnetic moments. Let $\mathbf{r}_i$ be the position vector of the ith electron, $\mathbf{r}_N$ the position vector of the nucleus in question, and further let $\mathbf{r}_{iN}$ be the vector joining the two. Let $\mathbf{H}_0$ be an externally applied magnetic field. The Hamiltonian representing the interaction between the nuclear moment μ_N and the internal and external fields is given by

$$\mathcal{H} = -g_N\beta_N\mathbf{I}\cdot\left\{\mathbf{H}_0 + \frac{8\pi}{3}\sum_i \boldsymbol{\mu}_i\delta(r_i - r_N) + \sum_i\left(\frac{\boldsymbol{\mu}_i}{r_{iN}^3} - \frac{(3\mathbf{r}_{iN}\mathbf{r}_{iN}\cdot\boldsymbol{\mu}_i)}{r_{iN}^5}\right)\right\} \quad (1\text{-}3)$$

where the sums are carried out over all the electrons and $\boldsymbol{\mu}_i = -g\beta\mathbf{S}_i$ is the magnetic moment of the ith electron ($g = 2$ and β is the Bohr magneton). The second term in the curley brackets is the operator which represents the field set up at the nucleus by the magnetic moment of electrons situated at the nucleus. This is the hyperfine, or contact interaction, first obtained by Fermi (2,3). This term is usually much larger than the third term, the dipole-dipole term, which represents the magnetic field set up by electrons which are at points removed from the nuclear position r_N.

It is vital to remember that the internal fields produced by the electrons in a metal, paramagnetic, ferromagnet, or antiferromagnet, fluctuate very rapidly compared to the Larmor frequency of the nuclei. Thus the nuclei respond only to the time-average of the field set up by the electrons, and the nuclear resonance frequency is shifted from $g_N\beta_N H_0/h$ by an amount $\nu_{\text{int}} = g_N\beta_N\langle H_{\text{int}}\rangle/h$. Thus

$$\nu = g_N\beta_N H_0/h + \nu_{\text{int}}$$

To determine $\langle H_{\text{int}}\rangle$ one must take a statistical average of the last two terms in equation (1-3) over the various stationary

states of the electronic system. The evaluation of this statistical average depends in detail on the nature of the solid under study. Nevertheless, since the local fields are proportional to the magnetic moment μ of the electrons, we can expect $\langle H_{\text{int}} \rangle$ to be proportional to the magnetization $M(T)$, which is a function of the temperature (T). Hence

$$\langle H_{\text{int}} \rangle = A'M(T) \tag{1-4}$$

In paramagnets M is proportional to H_0. In feebly paramagnetic metals $\langle H_{\text{int}} \rangle / H_0$ is the Knight shift. In ferromagnets and antiferromagnets there is a spontaneous internal magnetization in zero external field, and the nuclear resonance can be observed in the absence of an external field.

A' contains information on the unpaired spin probability density for electrons at the nucleus. (Two electrons which have the same spacial wave functions and differ only in spin states are called *paired* electrons. These have no net spin magnetic moment, and hence make no contribution to $\mathcal{H}$.) A' also contains information on the dipole sum in equation (1-3). We therefore see that the shift

$$\nu_{\text{int}} = AM(T) \tag{1-5}$$

of the nuclear resonance frequency away from $\nu_0 = g_N \beta_N H_0 / h$ presents us with information jointly on the electronic wave function and on the magnetization, M.

It is clear from equation (1-5) that studies of the pressure-dependence of the internal fields, when combined with measurements of the compressibility $(1/V)(\partial V/\partial P)_T$, can provide information on the volume-dependence of the coupling constant and the volume-dependence of the magnetization, since

$$(\partial \ln \nu_{\text{int}}/\partial \ln V) = (\partial \ln \nu_{\text{int}}/\partial P)_T/(1/V)(\partial V/\partial P)_T \tag{1-6a}$$

$$= (\partial \ln A/\partial \ln V)_T + (\partial \ln M/\partial \ln V)_T \tag{b}$$

The volume-dependence of A contains information on the alteration of the electronic wave functions as the atoms in the

solid are brought closer together. The volume-dependence of the magnetization, taken at different temperatures, contains information on such quantities as the volume-dependence of the Curie, or Neel, temperature, and the volume-dependence of the saturation magnetization.

A more subtle, but nonetheless important, application of measurements of the pressure-dependence of ν_{int} is in correcting measurements of the temperature-dependence of ν_{int} for the effects of thermal expansion. In using equation (1-5) to obtain accurate information on the temperature-dependence of the magnetization it must be kept in mind that comparison with theory requires measurements of ν_{int} to be made without change in the size of the unit cell. Since measurements of ν_{int} are made at constant pressure, thermal expansion alters the size of the unit cell. This effect can be corrected using the pressure measurements. For simplicity, let us assume that we deal with a cubic crystal in which the dimensions of the unit cell and the positions of atoms inside it can be specified by a single parameter which, we shall take as the volume (V) of the unit cell. In this case the relation between constant-pressure and constant-volume measurements of the temperature-dependence of ν_{int} is given by

$$(\partial \ln \nu_{\text{int}}/\partial T)_V = (\partial \ln \nu_{\text{int}}/\partial T)_P - (\partial \ln \nu_{\text{int}}/\partial \ln V)_T(\partial \ln V/\partial T)_P \quad (1\text{-}7)$$

The last term in equation (1-7) is the effect of the thermal expansion. The magnitude of this term depends on the size of the thermal expansion coefficient and the volume-dependence of ν_{int}. This latter quantity can be obtained from the pressure-dependence of ν_{int} by equation (1-6a). Thus, if the compressibility $(1/V)(\partial V/\partial P)_T$ is known at various temperatures, measurements of the pressure-dependence of the internal field enables the determination of $(\partial \ln \nu_{\text{int}}/\partial \ln V)$ and hence the volume expansion correction in equation (1-7). Pressure measurements are necessary, as we see, in making the magnetic equivalent of the famous C_P to C_V corrections in the theory of specific heats.

The electrons, too, serve as probes for the internal fields in a solid. In Section 1.5 of this chapter we deal with the measurement of the pressure-dependence of the hyperfine interaction constant between the electrons and nucleus of paramagnetic ions substituted into various host lattices.

1.2 Feebly Paramagnetic Metals (The Knight Shift)

The magnetic field at the nucleus of an atom in a nonferromagnetic metal can be determined from the Hamiltonian (equation (1-3)), provided that the stationary states of the electrons are known. In a metal the electrons often can be unambiguously separated into two groups—the core electrons, and the conduction electrons. The core electrons nominally consist of electrons with spins paired off in spherically-symmetrical closed shells. Such electrons make no contribution to the field at the nucleus. The valence electrons are distributed throughout the metal in spin-up and spin-down Bloch states, and electrons occupy these states in accordance with the Fermi-Dirac statistics.

It is necessary at the outset to estimate the correlation time, τ_c, for fluctuations in the field at the nucleus set up by the conduction electrons. Because of the Fermi statistics it is necessary to consider only those electrons near the Fermi surface. The conduction electrons well below this energy have their spins completely paired. The electrons near the Fermi surface have a velocity v_F and jump from one unit cell to another in a time $\tau_c \sim a/v_F \sim \hbar/\zeta$ where a is roughly the edge length of the unit cell, and ζ is the Fermi energy. It is this jumping from one atom to another which produces the fluctuation of the field at the nucleus. The correlation time, $\tau_c \sim 10^{-16}$ sec, is much shorter than the inverse of the Larmor frequency ($1/\nu_L \sim 10^{-7}$ sec) of the nucleus. As a result, we see at the outset that the field at the nucleus must be calculated by taking the statistical average of the term in curly brackets in the Hamiltonian (equation (1-3)).

To carry out the statistical averaging, we introduce the density of conduction band states, $n(\epsilon)$, around the energy ϵ, and the Fermi function, $f_0(\epsilon - \zeta/kT)$. In the presence of a magnetic

field it is convenient to divide the density of states into moment-up and moment-down ($n^+(\epsilon)$ and $n^-(\epsilon)$) parts. It is also necessary to include in the argument of the Fermi function the potential energy $\pm\beta H_0$ of the electrons. If we now define N^+ and N^- as the total number of electrons with moments respectively parallel and antiparallel to the applied field, then the relation

$$N = N^+ + N^- = \int_0^\infty \left[n^+(\epsilon) f_0 \left(\frac{\epsilon - \beta H_0 - \zeta}{kT} \right) + n^-(\epsilon) f_0 \left(\frac{\epsilon + \beta H_0 - \zeta}{kT} \right) \right] d\epsilon \quad (1\text{-}8)$$

determines the Fermi level ζ. By expanding the Fermi function in powers of $\beta H_0/kT$ it is seen that to first order the Fermi level is unaffected by the application of a magnetic field. To carry out the statistical average of the magnetic field at the nucleus (H_N) we observe that for cubic metals the dipole-dipole terms in equation (1-3) give no contribution. The hyperfine interaction term gives a contribution only for the conduction electrons, and we obtain

$$H_N = H_0 + \frac{8\pi}{3} \int_0^\infty \left| \Psi(r_N, \epsilon) \right|^2 \beta \left[n^+(\epsilon) f_0 \left(\frac{\epsilon - \beta H_0 - \zeta}{kT} \right) - n^-(\epsilon) f_0 \left(\frac{\epsilon + \beta H_0 - \zeta}{kT} \right) \right] d\epsilon \quad (1\text{-}9)$$

The quantity in square brackets is zero, except for a narrow range of the order of kT near the Fermi energy ζ. Thus if $|\Psi(r_N, \epsilon)|^2$ is a slowly-varying function of the energy ϵ, we may remove it from the integral and set $\epsilon = \zeta$ in its argument. The terms that remain inside the integral give exactly the magnetic moment $M = \chi_P H_0$.

$$M = \beta(N^+ - N^-) = \beta \int_0^\infty \left[n^+(\epsilon) f_0 \left(\frac{\epsilon - \beta H_0 - \zeta}{kT} \right) - n^-(\epsilon) f_0 \left(\frac{\epsilon + \beta H_0 - \zeta}{kT} \right) d\epsilon \right. \quad (1\text{-}10)$$

Thus we may write

$$H_N = H_0 + \frac{8\pi}{3} \chi_P |\Psi(r_N, \vartheta)|^2 H_0 = H_0(1 + K) \quad (1\text{-}11)$$

The Knight shift K may be written as

$$K = (8\pi/3)(\chi_P \Omega P_F) \quad (1\text{-}12)$$

where all the quantities entering into equation (1-12) have been normalized per atom. χ_P is the magnetic susceptibility per unit volume, Ω is the volume per atom, and $P_F \equiv |\Psi(r_N, \zeta)|^2$ where Ψ is normalized over the unit cell. The quantity $\chi_P \Omega$ is the paramagnetic susceptibility per atom, given in the free-electron model by the Pauli expression

$$\chi_P \Omega = 3\beta^2 p / 2\zeta \quad (1\text{-}13)$$

where $p \equiv$ number of valence electrons per atom. It will be observed that the contribution to the resonance frequency which comes from the internal field is exactly of the form of equation (1-5), *viz.*

$$\nu_{\text{int}} = (g_N \beta_N / h) K H_0 = (g_N \beta_N / h)(8\pi/3) P_F (\chi_P \Omega H_0) \quad (1\text{-}14)$$

where P_F plays the role of the coupling constant and $\chi_P \Omega H_0$ is the magnetization, M, per atom.

Before turning to the measurement of the pressure-dependence of K, it is well that we consider an important effect that occurs again and again in the study of the hyperfine interaction, namely core polarization (4,5). We have heretofore explicitly assumed that the core electrons are distributed in orbitals in which the spins are exactly paired off, i.e. for each electron in a spin-up state there is another in an identical spin-down state. This assumption will be correct if there are equal numbers of spin-up

and spin-down electrons in the system under consideration. However, in magnetic materials this is not the case. As Slater has emphasized (6) the existence of a net spin in the system means that a spin-up electron (in our case a spin-up core electron) will see a different exchange potential than will a spin-down electron. The result is that spin-up and spin-down core electrons will have slightly different orbitals and, in particular, the spin-up and spin-down probability densities at the nucleus will not be identical. Thus the core electrons are polarized by the exchange interaction with the magnetic electrons and contribute to the total unpaired spin density at the nucleus. No explicit (7) calculations have yet been made for the effects of core polarization on the Knight shift in metals. Nonetheless, we must keep in mind that P_F as deduced from the Knight shift does contain contributions from core electrons polarized by exchange interaction with magnetic electrons at the Fermi level ζ.

The pressure-dependence of K has been measured (8) in lithium, sodium, rubidium, cesium, copper, and aluminum at room temperature over the pressure range 1 to 10,000 kg/cm^2. The measurements consist of the determination of the change in nuclear resonance frequency ν when hydrostatic pressure is applied to a sample placed in a constant external field, H_0. If $\nu(P)$ and $\nu(0)$ are respectively the nuclear resonance frequencies at pressure P and at 1 atmosphere it follows from equations (1-2) and (1-11) that

$$K(P) - K(0) = \frac{\nu(P) - \nu(0)}{\nu(0)} (1 + K(0)) \qquad (1\text{-}15)$$

Thus, measurement of the pressure-dependence of K requires the determination of the change in nuclear resonance frequency on applying the pressure, and the values of K at atmospheric pressure. The latter quantities are well known (9). The changes in ν however are very small in the cases of lithium and sodium. At 10,000 kg/cm^2, the change in ν is only $\sim$30 cps for lithium and 110 cps for sodium. Hence, stringent requirements are placed on stabilization of the external field and the frequency stability

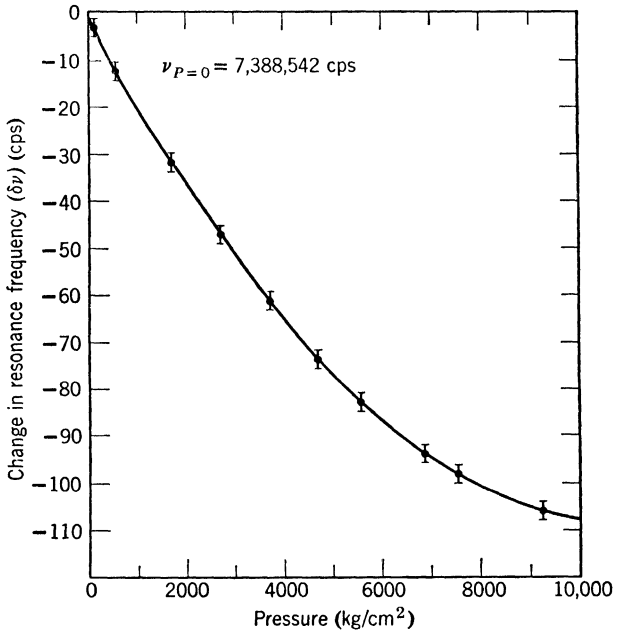

Figure 1. The change in the Na^{23} nuclear resonance frequency as a function of pressure at 24.4°C. The accuracy of the determination of the Na frequency is ± 1 cps at each pressure.

of the spectrometer. To meet these requirements, a system, then unprecedented in accuracy, was developed which enabled stabilization of both spectrometer frequency and magnetic field to a few parts in 10^7 over long periods of time (8 to 10 hours). The results for sodium are shown in Figure 1. It will be noted that the center of the resonance line is determined to within ±1 cps at each pressure. When the results for the pressure dependence of K are combined with Bridgman's measurements of the volume compression of the solid we obtain the volume-dependence of K.

The primary object of the measurement of the volume-dependence of K was the determination of the volume-dependence

of P_F. This may be obtained from the volume-dependence of the Knight shift, provided that the volume-dependence of $\chi_P\Omega$ is known. Clearly it would be most desirable to make an independent experimental measurement of the volume-dependence of the Pauli susceptibility. Unfortunately, however, the experimental accuracy now available for measurements (10) of χ_P are too low to permit determination of its volume-dependence. Instead, the collective electron picture of Pines (11), which is successful in predicting quantitatively χ_P at atmospheric pressure, was used to *calculate* the volume-dependence of $\chi_P\Omega$. Combining this with the measurements of K vs. volume, the volume-dependence of P_F was deduced and compared with the theoretical predictions of W. Kohn and F. Ham and H. Brooks. The quantum defect method developed by Brooks and Ham (12) permits calculation of the volume-dependence of P_F for all the alkali metals without explicit construction of the potential in which the conduction electrons move. This theory gives very good results (8) for the volume-dependence of P_F for sodium and rubidium. Cesium shows a much stronger volume-dependence than is predicted by the theory. Because of convergence difficulties the theory gives no prediction for lithium. These results are summarized in Table I-1.

The temperature-dependence of K is also of interest. McGarvey and Gutowsky (13) measured K vs. the temperature (T) for Li, Na, Rb, Cs. They believed that the temperature-dependence was due entirely to the thermal expansion: that K was not an *ex-*

Table I-1
The Fractional Change in the Knight Shift and P_F on Changing the Volume of the Solid by the Fraction ($\Delta V/V$)

Metal	$\Delta V/V$	$\Delta K/K$	$\Delta P_F/P_F$	$\Delta P_F/P_F$ (theoretical)
Lithium	−0.08	−0 0116	−0.005	
Sodium	−0.13	−0.0131	+0.072	+0.062
Rubidium	−0.23	+0.068	+0.22	+0.21
Cesium	−0.24	+0.415	+0.57	+0.34

plicit function of the temperature. In terms of equation (1-7), in which ν_{int} is replaced by K, they believed that $(\partial \ln K/\partial T)_V = 0$. The availability of the pressure measurements discussed above enables the determination of $(\partial \ln K/\partial \ln V)_T$. When this is combined with the known thermal expansion $(\partial \ln V/\partial T)_P$ and compared to $(\partial \ln K/\partial T)_P$, it is found that K is an explicit function of the temperature at constant volume. It was proposed (8,8a) that this effect is due to the modulation of P_F by the lattice vibrations. These vibrations cause a fluctuation of the volume Ω of the unit cell, and a concomitant fluctuation in the value of P_F. The susceptibility per atom $\chi_P\Omega$ does not follow the very rapid fluctuation because the time required for a spin flip is long compared to the characteristic period of the lattice vibrations. The nucleus therefore responds to the time-average value of P_F, which is

$$\overline{P_F(\Omega)} \cong P_F(\Omega_0) + {}^1/_2(\partial^2 P_F/\partial\Omega^2)\overline{(\Omega - \Omega_0)^2} \qquad (1\text{-}16)$$

The magnitude and temperature-dependence of $\overline{(\Omega - \Omega_0)^2}$ can be computed using the Debye model of lattice vibrations, while $\partial^2 P_F/\partial\Omega^2$ can be obtained from the volume-dependence of P_F as deduced from the pressure-dependence of K. Calculations (8) using this model are in good agreement with the experimental results.

1.3 Antiferromagnets

Manganous fluoride, MnF_2, is a nearly ionic crystal. On forming the crystal lattice, in first approximation, the manganese atoms become doubly-ionized, magnetic, Mn^{2+} ions with the configuration $^6S_{5/2}$, while the fluorine atoms become singly-charged nonmagnetic F^- ions in the closed shell configuration $^1S_0$. The magnetic moments on the Mn^{2+} sites are responsible for the paramagnetism of MnF_2 at temperatures above the Neel temperature, T_N. Below T_N the superexchange interaction and anisotropy fields produce an antiferromagnetic ordering of the Mn^{2+} spins. In Figure 2 we see the arrangement of nearest-

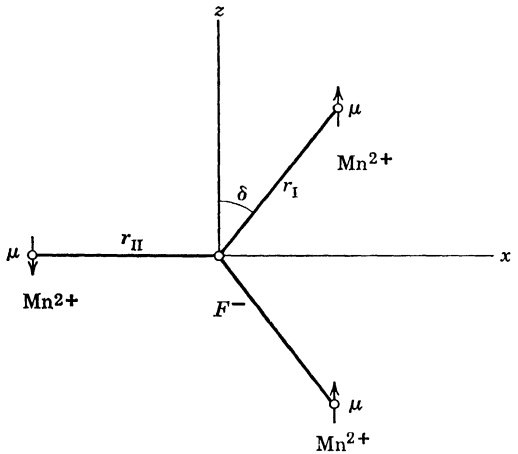

Figure 2. The arrangement of nearest-neighbor Mn^{2+} ions around a fluorine nucleus in MnF_2. The arrows represent the magnitude and relative orientation of the time-averaged magnetic moment of the Mn^{2+} ions. A second-type fluorine site sees the same configuration as above, except that the direction of the Mn^{2+} spins are reversed.

neighbor Mn^{2+} spins around each fluorine site. The nucleus under study is the F^{19} nucleus. In this crystal there are two types of fluorine sites. In the antiferromagnetic state, one type of fluorine sees the spin arrangement shown in Figure 2, while the other type sees a reversed orientation of manganese spins.

To examine the magnetic effect of the near-neighbor Mn^{2+} spins on the F^{19} nucleus we employ the Heitler-London, or atomic orbital, description of the wave functions in the crystal. If we neglect entirely the effect of overlap between the fluorine and manganese orbitals, then we may expect that the field (H) that the fluorine nucleus sees is due entirely to the magnetic dipole field of the Mn^{2+} ions. At T = 0° K, in the case of complete antiparallel alignment, this would produce a magnetic field of 12,500 gauss, 12,800 of which is due to the nearest-neighbor ions and −300 of which is contributed by the further neighbors. V. Jaccarino and R. G. Shulman (14), who were the first

to observe the F^{19} nuclear resonance in MnF_2, found that at $T \simeq 0°$ K, the magnetic field at the fluorine site was actually 40,470 gauss. They proposed (15) that this large field was due to an indirect hyperfine interaction between the spin of the Mn^{2+} ions and the F^{19} nucleus, and suggested the possibility that the observed hyperfine interaction was the result of covalent bonding between the fluorine ion and its Mn^{2+} neighbors. The covalent bonding requires a transfer of fluorine electrons onto the manganese neighbors. The transferred electrons must have their spins antiparallel to those on the Mn^{2+} neighbors, since each of these already has its full complement of 5 parallel spins. The unpaired spins remaining on the F^- ion then interact with the F^{19} nucleus through the hyperfine interaction. Despite this suggestion the origin of the Mn-F hyperfine interaction was not clearly established at this stage in the development of the subject.

Turning now to the situation at temperatures above 0° K, we must examine the correlation time (τ_c) for fluctuations of the Mn^{2+} spins. This correlation time is determined by the Mn-Mn superexchange interaction which couples each pair of Mn^{2+} ions in accordance with $\mathcal{H}_{12} = J\mathbf{S}_1 \cdot \mathbf{S}_2$. Fluctuations between the two degenerate states $(1\uparrow)$, $(2\downarrow)$ and $(1\downarrow)$, $(2\uparrow)$ take place with a frequency $\omega_e \sim J/\hbar$. Estimating the exchange integral J from the Neel temperature $kT_N \sim J$, we have $\omega_e \sim kT_N/\hbar$. Using $T_N \simeq 68°$ K (16) we find $\omega_e \sim 8 \times 10^{12}$/sec and $\tau_c = 2\pi/\omega_e \sim .8 \times 10^{-12}$ sec. Clearly this is much shorter than the inverse of the Larmor frequency of the fluorine nucleus, so again we see that the nucleus responds only to the time-average spin orientation of the neighbor manganese spins. This time-average spin orientation, in turn, is proportional to the sublattice magnetization, $M(T)$. Thus we may write that the resonance frequency, ν, is related to the sublattice magnetization by

$$\nu = AM(T) \tag{1-17}$$

which of course is identical in form with equation (1-5). The constant of proportionality, A, in equation (1-17) includes both

the hyperfine coupling constant and the dipole-dipole interaction.

At temperatures well below the Neel temperature, $M(T)$ becomes a constant independent of the temperature and very nearly independent of the volume. Thus, by measurements of the pressure-dependence of the resonance frequency ν at very low temperatures and in zero external field, one can determine the pressure-dependence of A, and hence the pressure-dependence of the hyperfine coupling constant. Furthermore, if the change in lattice dimensions produced by the pressure is known, one may determine how the hyperfine coupling constant depends on the distance between the manganese and fluorine ions. This experiment has been performed (17) at 4.2° K using liquid helium as a pressure-transmitting medium. The pressure range was limited to only 100 kg/cm^2, but the accuracy with which the line center could be determined was sufficient to specify that

$$(1/A)(\partial A/\partial P) = (1.9 \pm 0.1) \times 10^{-6}/(\text{kg/cm}^2)$$

At higher temperatures, where $M(T)$ is not a constant, the pressure-dependence of ν arises not only out of the pressure-dependence of A, but also out of the pressure-dependence of the magnetization, the sublattice magnetization being a function of pressure through its dependence on the Neel temperature T_N. We may therefore write

$$(1/\nu)(\partial\nu/\partial P)_T = (1/A)(\partial A/\partial P)_T + (1/M)(\partial M/\partial T_N)(\partial T_N/\partial P) \quad (1\text{-}18)$$

If we take $M = M(T/T_N)$ as the functional form of the dependence of M on T and T_N, it follows that

$$(1/\nu)(\partial\nu/\partial P)_T = (1/A)(\partial A/\partial P)_T - (T/T_N)(\partial \ln M/\partial T)_{T_N}(\partial T_N/\partial P) \quad (1\text{-}19)$$

Since $(\partial \ln M/\partial T)_{T_N} \cong (\partial \ln \nu/\partial T)_P$, we may obtain (dT_N/dP) by measuring the pressure-dependence of ν at a temperature at which the second term on the right-hand side of equation (1-19) is appreciable compared to the first. This measurement has been carried out at 35.7° K, yielding a determination of

$$(dT_N/dP) = (0.298 \pm 0.02) \times 10^{-3} \text{ °K/(kg/cm}^2\text{)}$$

using $T_N \simeq 68.5°$ K. As a check of self-consistency, we can measure $(1/\nu)(\partial\nu/\partial P)_T$ at some other temperature and compare the result with the prediction of equation (1-19) obtained using the values of $\partial \ln A/\partial P$ and $\partial \ln T_N/\partial P$ given above. At 20°K equation (1-19) predicts $(1/\nu)(\partial\nu/\partial P)_T = (2.2 \pm 0.1) \times 10^{-6}$/(kg/cm^2) whereas we found $(2.21 \pm 0.04) \times 10^{-6}$/(kg/cm^2). This satisfactory agreement lends support to the use of equation (1-19).

Recently (18) the pressure-dependence of the Neel temperature in MnF_2 has been determined very accurately by making use of the fact that at the Neel temperature the F^{19} nuclear resonance line width broadens so drastically that the line intensity falls beneath the noise. Any change in the temperature at which this disappearance takes place could be detected to within 2 millidegrees. By measuring the pressure-dependence of the disappearance temperature we have found

$$(dT_N/dP) = (0.302 \pm .002) \times 10^{-3} \text{ °K/(kg/cm}^2\text{)}$$

which is in excellent agreement with the results obtained above. With the aid of measurements of the compressibility of MnF_2, these determinations of dT_N/dP show how the superexchange interaction between Mn^{2+} ions depends on the distances and angles which characterize the Mn-F-Mn geometry. No theoretical calculations have yet been made to predict the dependence of the superexchange integral on the Mn-F-Mn distances and angles.

On the other hand, a theory has been proposed (17,19,20) to account for the magnitude and pressure-dependence of the hyperfine interaction between manganese ions and the fluorine

nucleus. In essence, this theory proposes that the unpairing of the core electrons in *s* states around the fluorine nucleus arises out of Pauli, or exchange, repulsion between fluorine and manganese spins which have the same orientation. Because of orthogonality, this exchange repulsion does not act on those fluorine electrons whose spin is antiparallel to the direction of the neighbor Mn^{2+} spin. As a result, spin-up and spin-down *s* and *p* orbitals around the fluorine nucleus are slightly different. The situation described here is physically quite similar to the core polarization effect mentioned in connection with the Knight shift. In the present case, the core is polarized by electrons whose orbitals are centered on sites different from the nucleus experiencing the hyperfine interaction. In the more familiar example (4,5,7) the core is polarized by unpaired electrons centered on the nucleus in question. Furthermore, in the present case, it is possible (17) to calculate the hyperfine interaction produced by the Pauli repulsion *kinematically* without constructing the exchange potentials and solving the unrestricted Hartree-Fock equations.

Using the model of Pauli or exchange repulsion first proposed by Mukherji and Das (20), along with W. Marshall's estimate of the alteration of the Hartree-Fock free-ion wave functions appropriate to the ions in the solid, calculations of the magnitude and pressure-dependence of A were made which were in excellent agreement with observation (17). This agreement lent support to the view that covalency effects were not important in impairing the *s* orbitals on the fluorine ion. However, subsequent refinements of the theory (19,21) showed that a cross-term between the $2s$ and $1s$ orbitals had been omitted in the original calculation (17). This term reduces the magnitude of the theoretical prediction of the hyperfine coupling constant by a factor of two. This difficulty may be due to inadequate knowledge of the details of the $3d$ Mn^{2+} orbitals, especially in the region near the fluorine ion. On the other hand, we must now realize that covalency may play a significant role in determining the hyperfine interaction.

1.4 Ferromagnets

By measurements of the Mossbauer effect in iron, Hanna *et al.* (22) have shown that the ground state ($I = {}^1/_2$) of the Fe^{57} nucleus in ferromagnetic iron is split at room temperature by about 45 mc due to the interaction between the small nuclear moment and the large (~330,000 gauss) magnetic field at the nuclear site. Following this observation Gossard, Portis, and Sandle (23) and Robert and Winter (24) observed this splitting directly by detecting the nuclear resonance of the Fe^{57} nucleus in the effective internal field (H).

In a pioneering paper, W. Marshall (25) presented a theory for the origin of the field at the nucleus. All the sources of the field in his theory fluctuate very rapidly compared to the Larmor frequency. Thus the nucleus responds to the time-average field from each source. In the case of iron, which is cubic, the following effects contribute to the total field at the nucleus:

(*1*) The demagnetizing field $-DM$, the Lorentz field, and the external field H_0. M is the magnetization in each domain.

(*2*) The field produced by hyperfine interaction with the 4*s* conduction electrons which are polarized by the ferromagnetically-aligned 3*d*-electrons.

(*3*) The field produced by the hyperfine interaction with 4*s*-electrons admixed into the 3*d*-band.

(*4*) The field produced by the orbital angular momentum of the 3*d*-electrons. Normally, the orbital angular momentum of these electrons is quenched by the crystallize electric fields. However, the spin-orbit coupling permits the ion to have a nonvanishing component of the orbital angular momentum if the spin is oriented. This orbital contribution to H is proportional to the time-average spin orientation, i.e., to the magnetization M.

(*5*) Finally, we have the contribution from the core polarization of the 3*s*-, 2*s*-, and 1*s*-electrons produced by the spin-aligned *d*-electrons.

The field at the nucleus has been found (26) to be in a direction *opposite* to that of the magnetization vector. Since (*5*) is a large negative effect, it is generally believed that the core polarization is by far the dominant effect in iron.

All the sources of the field considered by Marshall are proportional to the mean spin per atom, and hence to the mag-

netization (M). Thus one concludes that the resonance frequency ν is proportional to the saturation magnetization as

$$\nu = AM \tag{1-20}$$

On the basis of equation (1-20) it was believed that precise measurements of the temperature-dependence of ν which were possible by measurements of the nuclear resonance frequency could be used to obtain very accurately the temperature-dependence of M. Naturally it was assumed that A was a constant independent of the temperature. Some doubt as to the validity of this basic assumption was raised by the results of Robert and Winter (24), who showed that at atmospheric pressure ν decreased more rapidly with temperature in the range 0 to 300° K than M (27). The French workers noted that ν could be expected to be a function of the temperature indirectly through the effect of the thermal expansion, and that different effects of the thermal expansion on M and ν might be responsible for the apparently different temperature-dependences of M and ν. They believed that if the temperature-dependences of these two quantities were corrected to constant volume, then $\nu(T)$ and $M(T)$ would be directly proportional. By making measurements of the pressure-dependence of ν and M at a number of different temperatures this supposition can be checked, since

$$(\partial\nu/\partial T)_V = (\partial\nu/\partial T)_P - (\partial\nu/\partial P)_T((V)(\partial P/\partial V))_T((1/V)(\partial V/\partial T)_P \tag{1-21}$$

Thus, if the compressibility, thermal expansion, and pressure-dependence of ν are known as a function of the temperature, equation (1-21) can be integrated to obtain $(\nu(T))_V$. A similar procedure holds for $M(T)$.

G. Benedek and J. Armstrong (28) have measured the pressure-dependence of the resonance frequency ν in ferromagnetic iron at −77° C, 0° C, and 84.2° C in the range 1 to 10,000 kg/cm^2. The results at 0° C are shown in Figure 3. It should be noted that at each pressure the Fe^{57} resonance frequency has been

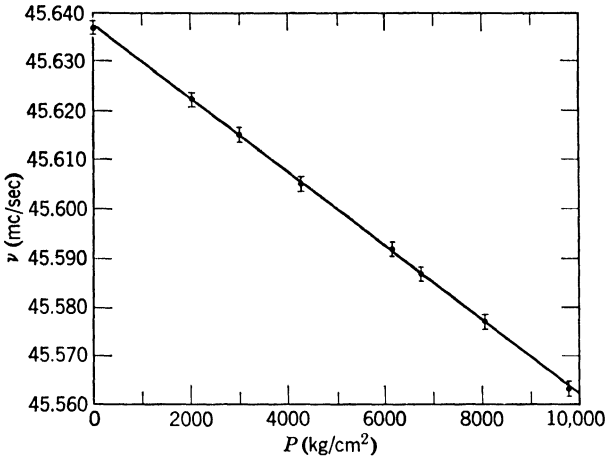

Figure 3. The Fe^{57} nuclear resonance frequency vs. pressure in ferromagnetic iron at 0°C.

measured to better than ±1 kc, while the line width was ~40 kc. It was found that $(1/\nu)(\partial\nu/\partial P)_T$ was nearly independent of the temperature and equal to

$$(1/\nu)(\partial\nu/\partial P)_{0°C} = (-1.64 \pm 0.01) \times 10^{-7}/(\text{kg/cm}^2)$$

Before applying these results to equation (1-21) to determine the temperature-dependence of ν at constant volume, we may briefly examine the source of the pressure-dependence of ν.

Since ν is nearly independent of the temperature, we have from equation (1-18) that

$$(1/\nu)(\partial\nu/\partial P) = (1/A_0)(\partial A_0/\partial P) + (1/M_0)(\partial M_0/\partial P) \quad (1\text{-}22)$$

where M_0 and A_0 are the values of M and A at $T = 0°$ K. We observe here a marked difference between the ferromagnetic and antiferromagnetic cases. In the case of MnF_2, the pressure-dependence of the sublattice magnetization arises out of the pressure-dependence of the Neel temperature T_N, and M_0 is a constant nearly independent of the pressure, being given es-

sentially by $2\beta S$ per atom (β is the Bohr magneton, S the spin quantum number). However, in the case of ferromagnetic metals each atom does not contribute an integral number of Bohr magnetons to the saturation magnetization. It is believed that this situation may arise out of an unequal distribution of electrons into spin-up and spin-down energy bands. Under these conditions we may expect that a change in the volume of the solid will alter the distribution of electrons in these bands and hence change M_0. In fact, J. S. Kouvel (29) and F. Galperin (30) have observed the pressure-dependence of M_0. As far as the dependence of M on the Curie temperature is concerned, we must remember that since $T_c \sim 1000°$ K, at 300° M is only weakly dependent upon T_c. Of course, if the temperature were raised higher we could obtain information about the pressure-dependence of T_c from the temperature-dependence of $\partial\nu/\partial P$. However, in the case of iron, L. Patrick's (31) measurements of dT_c/dP show that the Curie temperature in iron is essentially independent of the pressure.

We may now use measurements of dM_0/dP to determine $(1/A_0)(\partial A_0/\partial P)$ from equation (1-22). J. Kouvel has found (29) that

$$(1/M_0)(\partial M_0/\partial P) = (-2.78 \pm 0.25) \times 10^{-7}/(\text{kg/cm}^2)$$

Thus we find $(1/A_0)(\partial A_0/\partial P) = (1.14 \pm 0.25) \times 10^{-7}/(\text{kg/cm}^2)$, or $\partial \ln A/\partial \ln V = -0.19$.

Returning now to equation (1-21), we may obtain $(\nu(T))_V$ from the known temperature-dependence of $(\partial\nu/\partial P)$, $(1/V)\cdot(\partial V/\partial T)$ and $V(dP/dV)$. By carrying out an exactly similar procedure we may also obtain $(M(T))_V$. The results for $(M(T))_V$ and $(\nu(T))_V$ are shown in Figure 4. It is clear that even when corrected to constant volume, ν and M are not directly proportional to one another, i.e. the coupling constant A is an explicit function of the temperature. In fact the experimental data indicate that the temperature-dependence of A is given by

$$A = A_0(1 - 0.77 \times 10^{-7}T^2) \qquad (1\text{-}23)$$

The T^2 temperature-dependence of A suggests a band description for the electrons responsible for the hyperfine interaction. In fact, Kittel has suggested (32) that the temperature-dependence of A may be due to the excitation of electrons higher

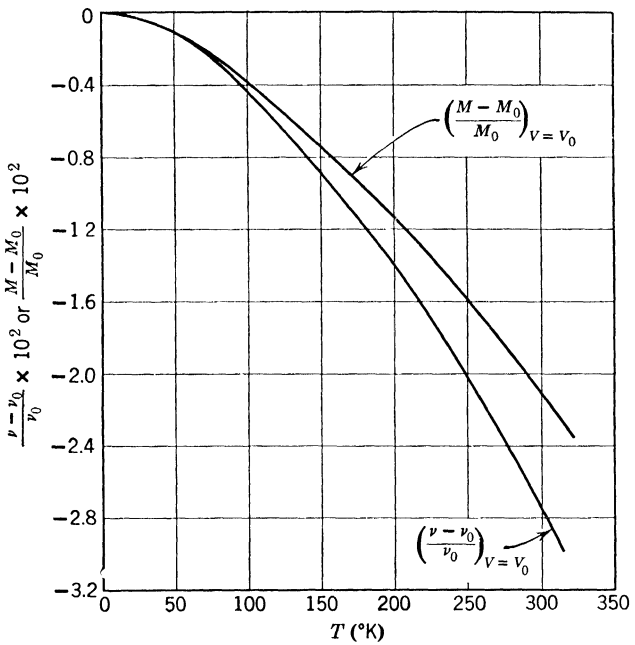

Figure 4. $(\nu - \nu_0)/\nu_0$ and $(M - M_0)/M_0$ in iron as a function of the temperature at constant volume, using Kouvel's data to remove the effect of thermal expansion on M.

into the d band as the temperature is increased. The effective nuclear field is the resultant effect of the hyperfine interaction with all the spin-up and spin-down d electrons, each of which has a different energy, ϵ, a different Bloch function, and hence a different coupling constant, $a(\epsilon)$. This band description is very similar to the situation that obtains in the Knight shift. We may write the resonance frequence ν as

$$\nu = \int_0^\infty n^+(\epsilon)a^+(\epsilon)f_0\left(\frac{\epsilon - k\theta'\sigma - \zeta}{kT}\right)d\epsilon - \int_0^\infty n^-(\epsilon)a^-(\epsilon)f_0\left(\frac{\epsilon + k\theta'\sigma - \zeta}{kT}\right)d\epsilon \qquad (1\text{-}24)$$

where $n^{\pm}(\epsilon)$ is the density of states at energy ϵ for electrons with moments either up or down relative to the Weiss internal field. In this equation $a^{\pm}(\epsilon)$ is the coupling constant which essentially gives the field at the nucleus set up indirectly by a d-electron with energy ϵ and moment parallel or antiparallel to the Weiss field; f_0 is the Fermi function which gives the probability that a given energy state will be occupied; ζ is the Fermi energy. We must of course include in the argument of f_0 the potential energy of the d-electron. This potential energy is written as $\pm k\theta'\sigma$, i.e., it is taken as proportional to the saturation magnetization $M = \beta\sigma$, where β = the Bohr magneton and

$$\sigma = \frac{N^+ - N^-}{N^+ + N^-} = \int_0^\infty n^+(\epsilon)f_0\left(\frac{\epsilon - k\theta'\sigma - \zeta}{kT}\right)d\epsilon - \int_0^\infty n^-(\epsilon)f_0\left(\frac{\epsilon + k\theta'\sigma - \zeta}{kT}\right)d\epsilon \qquad (1\text{-}25)$$

It is to be noted that the expression for σ is very similar to that for ν. In fact if the coupling constant $a(\epsilon)$ were independent of energy we would immediately have $\nu = aM/\beta$. Thus in the present theory the temperature-dependence of A results from the energy-dependence of the coupling constant $a(\epsilon)$. In general we may look upon equation (1-25) as an equation for σ in terms of ζ and T. A second equation for σ, ζ, and T is given by the normalization condition

$$1 = \frac{N^+ + N^-}{N^+ + N^-} = \int_0^\infty n^+(\epsilon)f_0\left(\frac{\epsilon - k\theta'\sigma - \zeta}{kT}\right)d\epsilon + \int_0^\infty n^-(\epsilon)f_0\left(\frac{\epsilon + k\theta'\sigma - \zeta}{kT}\right)d\epsilon \qquad (1\text{-}26)$$

Equations (1-25) and (1-26) suffice in principle to determine σ and ζ as functions of the temperature. In fact these equations with $n^+(\epsilon) \sim \epsilon^{1/2}$ are the basis of Stoner's "collective electron" model for the d electrons in a ferromagnet. The insertion of ζ as a function of σ and T as determined from equations (1-25) and (1-26) into equation (1-24) permits a determination of the dependence of ν on σ and the temperature. This procedure has been carried out explicitly (28) under a number of simplifying assumptions, *viz.* $n^+(\epsilon) = n^-(\epsilon)$, $a^+(\epsilon) = a^-(\epsilon)$. The result gives $\nu = A\sigma = AM/\beta$, with A containing a term in T^2 as the leading term in the power-series expansion of the temperature-dependence of A. As yet it has not been possible to reliably evaluate the coefficient of this T^2 term because of an absence of information on the energy-dependence of $a(\epsilon)$ and $n(\epsilon)$. Thus, at this point it is not possible to determine whether this theory is capable of accounting *quantitatively* for the observed temperature-dependence of the hyperfine coupling constant.

However, the present theory does provide at least qualitatively an explanation for the observed temperature-dependence of A in the following way. The observed constant is the average of contributions from d electrons distributed throughout the d band. It should be remembered though that d electrons at the bottom of the band and those at the top have very different radial distributions, and hence each of these produce quite different fields at the nucleus. As the temperature is increased the tail of the Fermi distribution rises higher into the d band, thereby bringing in contributions from states with coupling constants different from the average. Since the number of states brought in is proportional to T^2, the average value of A is altered by an amount proportional to T^2.

Kushida has recently measured (34) the pressure-dependence of the resonance frequency of the Ni^{16} nucleus in ferromagnetic nickel at 273° K and 372° K. He found that the frequency increases very strongly on increasing the pressure, and that

$$(1/\nu)(\partial\nu/\partial P)_{0°C} = +9.20 \times 10^{-7}/(\text{kg/cm}^2)$$

When this result is incorporated with a determination of the pressure-dependence of M for nickel, it will be possible to determine the temperature-dependence of the hyperfine coupling constant A in this ferromagnet as well as in iron. Kushida (35) has also studied the pressure-dependence of the nuclear resonance frequencies of the constituent nuclei in alloy systems like the Co^{59} resonance in cobalt-rich alloys with Fe, Ni, Cu, Cr, Mn, Al, or the Fe^{57} resonance in iron-rich alloys. Also, the Cu^{65} and Cu^{35} resonances have been observed in ferromagnetic Fe and Co alloys.

In a ferromagnet the magnetic field in which the nucleus precesses is provided by the aligned electron spins within the solid. No external magnetic field is required. Under these conditions it would seem possible to carry out nuclear resonance experiments in the pressure range of 100 kilobars with the aid of recently developed "superpressure" presses. Such an experiment has been successfully carried out by J. D. Litster and G. B. Benedek (35a). The Fe^{57} nuclear resonance frequency in natural-abundance iron was measured as a function of pressure to 65 kilobars. The upper pressure limit in this experiment was set by the strength of the press employed. The sample was iron powder whose particle size was $\sim$10 to 20 microns. This powder was dispersed in high dilution AgCl powder, which served as the pressure-transmitting medium. The absence of appreciable line-broadening above 15 kilobars indicated that for our sample geometry the pressure was transmitted essentially hydrostatically by the AgCl. The nuclear resonance frequency (ν) varies linearly with the pressure to 60 kilobars with

$$(\partial\nu/\partial P)_{20°C} = -7.67 \pm 0.22 \text{ (kc/kbar)}$$

This result is in agreement with the data of Armstrong and Benedek discussed above. The linear variation of ν with pressure suggests that the nuclear resonance frequency in iron can serve as a continuous pressure gauge at least up to 60,000 bars. The success of this experiment opens the way to nuclear resonance experiments in other ferromagnets, ferrimag-

nets, antiferromagnets, and those solids which exhibit pure quadrupole resonance. Such experiments should be particularly useful in detecting and elucidating the changes in electronic structure associated with high-pressure phase transitions.

1.5 Paramagnetic Ions in Crystals

Until this point we have looked upon the *nucleus* as the probe of the magnetic fields produced by the electrons in a solid. However the electrons themselves may be looked upon as probes since they have magnetic moments which interact with the fields set up by other electrons and nuclei. If individual magnetic ions are isolated by substituting them in very low concentration into a nonmagnetic host lattice, the ionic magnetic moments will interact primarily with the *magnetic* field set up by their own nuclei and the *electric* field produced by the surrounding nonmagnetic ions. Our attention in this section will be devoted largely to the former interaction; the effects of the crystalline electric field will be treated more fully in Section 2 of this chapter. The effect of the nucleus on the electron resonance frequency of the ion may be determined if we observe that the frequency ($\sim 1/T_2$) with which the nucleus jumps back and forth among its magnetic sublevels is generally much lower than the frequency $\nu_{\text{hyp}} = ((\Delta E)_{\text{hyp}}/h)$ corresponding to the hyperfine interaction energy. Thus the electron resonance line will be split into several hyperfine components, each corresponding to a particular orientation of the nuclear spin. By measuring the spacing of these hyperfine components the hyperfine interaction constant between the nucleus and electron may be obtained directly.

W. M. Walsh has studied the pressure-dependence of the hyperfine interaction for the S-state ion Mn^{2+} using the cubic crystals MgO and ZnS as host lattices. The impurity ion enters the lattice substitutionally for Mg and Zn respectively. The spin Hamiltonian which describes these ions is

$$\mathcal{H} = g\beta \mathbf{S}\cdot\mathbf{H} + A\mathbf{I}\cdot\mathbf{S} + (a/6)(S_x^4 + S_y^4 + S_z^4) \quad (1\text{-}27)$$

The first term describes the interaction between the magnetic moment of the 5 aligned electron spins ($S = 5/2$ for Fe^{3+} and Mn^{2+}) and the applied field H. The second term represents the hyperfine interaction between the nuclear spin **I** and the electron spin **S**. The final term describes the orienting action of the cubic crystalline potential on the spin angular momentum. This last term is roughly 10 times smaller than the hyperfine interaction term. We shall suppress it temporarily and consider the electron resonance spectrum that arises out of the first two terms in equation (1-27). In high magnetic fields (i.e., $A/g\beta H \ll 1$) we may describe the nuclear-electron system in terms of the quantum numbers I, S, m_I, and m_S. The eigenvalues of $\mathfrak{H}$ are readily calculated to the second order in the perturbation A to be

$$E(I, S, m_I, m_S) = g\beta H m_S + A m_I m_S + \frac{A^2}{2g\beta H}\{m_S(I(I+1) - m_I^2) - m_I(S(S+1) - m_S^2)\} \quad (1\text{-}28)$$

equation (1-28) shows, to second order in A, how the Zeeman levels of the electrons are split into $2I + 1$ levels by the hyperfine interaction. If a microwave magnetic field is applied perpendicular to the large field H, transitions can occur between levels satisfying the selection rules $\Delta m_S = \pm 1$ and $\Delta m_I = 0$. Since the spectrometer frequency ν_0 is normally kept constant while the magnetic field H is swept, resonant absorption takes place for those fields $H(m_I, m_S)$ which satisfy the condition

$$h\nu_0 = E(m_S, m_I) - E(m_S - 1, m_I)$$

$$h\nu_0 = g\beta H(m_I, m_S) + A m_I + \frac{(A^2/2g\beta)\{I(I+1) - m_I^2 - m_I(2m_S - 1)\}}{H(m_I, m_S)} \quad (1\text{-}29)$$

In general the solution of this equation for $H(m_I, m_S)$ involves a quadratic equation. However, if we keep in mind the fact that the last term is very small compared to the previous terms, we may to a good approximation replace $H(m_I, m_S)$ in the de-

nominator of the last term by the first order solution of equation (1-29), i.e. by $(h\nu_0 - Am_I)/g\beta$. Thus we have the explicit relation for the field at which resonant absorption can occur

$$H(m_I, m_S) \cong \frac{1}{g\beta}\left[h\nu_0 - Am_I - \frac{A^2}{2(h\nu_0 - Am_I)}\{I(I+1) - m_I^2 - m_I(2m_S - 1)\}\right]$$

The last term above shows that each absorption corresponding to a given m_I is further split into $(2S + 1)$ absorption lines in second order. Actually, the cubic crystalline field term of magnitude a also splits each hyperfine line into $(2S + 1)$ levels. The method for carrying out the detailed identification of each absorption line in terms of (m_I, m_S) is given in Mattarese and Kikuchi (37), who include the effect of the crystal field term. Once the various lines have been labelled in terms of m_S and m_I, the values of g, A, and a can be obtained immediately from the values of field at which absorption occurs.

By measuring the effect of hydrostatic pressure on the paramagnetic resonance spectrum of Mn^{2+} in MgO and ZnS, W. M. Walsh (36) has determined the pressure-dependence of the hyperfine coupling constant. In MgO he found that $A = -81.11 \times 10^{-4}$ cm^{-1} and $(1/A)(\partial A/\partial P)_T = -0.035 \times 10^{-6}/$-(kg/cm^2). Using the compressibility of MgO to determine the dependence of A on the volume V of the unit cell, he found that $(\partial \ln A/\partial \ln V)_T = +0.06$. On the other hand, in the case of ZnS the coupling constant is a much stronger function of the pressure. In this case $A = -63.73 \times 10^{-4}$ cm^{-1}, $(1/A)(\partial A/\partial P) = -0.44 \times 10^{-6}/(\text{kg/cm}^2)$, and $\partial \ln A / \partial \ln V = +0.35$.

The hyperfine coupling between the d electrons and the nucleus results from the "exchange polarization" of the core s electrons by the spins in the d orbitals. This is, of course, the same mechanism that we have discussed previously. The degree of polarization of the s electrons depends in detail on the radial distribution of the d wave function (38). On compression this

radial distribution is altered through the interaction of the d electrons with the neighbor ions, and hence A changes. In ZnS the relatively strong pressure-dependence of A, coupled with the low magnitude of A, indicates a strong interaction of the Mn orbitals with their neighbors, as is consistent with the covalent nature of this crystal.

1.6 Ferrimagnets

The effect of hydrostatic compression on the magnetization of ferrimagnets has been studied by R. V. Jones and I. P. Kaminow (39) using electron spin resonance techniques. To measure the pressure-dependence of the magnetization they placed a spherical sample in a microwave cavity in such a way that a number of different precessional modes of the magnetization can be excited by the microwave field. By orienting the external magnetic field so as to excite first one mode and then another one can determine (40,41) the magnetic moment M per unit volume $M = (N\mu/V)$ where μ is the moment per formula unit. The magnetic moment measured in this way is, of course, the total of contributions from all the sublattices. Using this technique, they studied the magnetization vs. pressure in the range from 1 to 10,000 kg/cm^2 for yttrium iron garnet, YIG, and for magnesium ferrite. They also obtained indirectly a value for the pressure-dependence of the erbium sublattice magnetization in erbium iron garnet, ErIG.

In YIG the yttrium ion is nonmagnetic, so that the magnetization comes from the iron sublattices. In this garnet they found that

$$\partial \ln \mu_{Fe}/\partial \ln V = -(0.57 \pm 0.03) \qquad (1\text{-}30)$$

In the erbium iron garnet Jones and Kaminow measured the pressure-dependence of the effective gyromagnetic ratio, g_{eff}, for the electrons. Under the assumption that Kittel's formula (42)

$$g_{eff} = g_{Fe}(1 + (M_{Fe}/M_{Er}))$$

holds, knowing the ratio M_{Fe}/M_{Er} and the volume-dependences of g_{Fe} and M_{Fe} (these may be obtained using the results on YIG), it is possible to determine the volume-dependence of M_{Er}. Carrying out this procedure, they found that

$$\partial \ln M_{Er}/\partial \ln V = -8.4 \tag{1-31}$$

Reasoning further that the magnetization of the erbium sublattice is proportional to the magnetization of the iron sublattice, the coupling constant being the product of $\lambda_{Er\text{-}Fe}$ (the iron-rare earth exchange constant) and the susceptibility χ_{Er} of the erbium lattice, one may write

$$M_{Er} = \chi_{Er}[\lambda_{Er\text{-}Fe}]M_{Fe} \tag{1-32}$$

Assuming that χ_{Er} is a constant, using equations (1-31) and (1-30) one finds

$$\partial \ln \lambda_{Er\text{-}Fe}/\partial \ln V \sim -7 \tag{1-33}$$

Thus the volume-dependence of the exchange coupling constant between rare earth and iron-ion lattices can be evaluated indirectly.

2. Electric Fields in Solids

2.1 Crystalline Electric Field Gradients: Nuclear Quadrupole Resonance in Ionic, Covalent, and Metallic Crystals.

Nuclei with spin I greater than $1/2$ can possess, in addition to a magnetic dipole moment, an electric quadrupole moment, Q. This quadrupole moment can then interact with the electric field gradient at the nuclear site to produce a sequence of energy levels. The Hamiltonian describing the interaction is

$$\mathcal{H}_Q = (eQ/2I(2I-1))\{\phi_{xx}I_x^2 + \phi_{yy}I_y^2 + \phi_{zz}I_z^2 + \phi_{xy}(I_xI_y + I_yI_x) + \phi_{xz}(I_xI_z + I_zI_x) + \phi_{yz}(I_yI_z + I_zI_y)\} \tag{2-1}$$

where

$$\phi_{ij} = (\partial^2 V(r)/\partial x_i \partial x_j)_{r = r_N}$$

In the above expression r_N = position of nucleus and $V(r)$ = electrostatic potential at the point r.

If the nucleus in question is at a site with axial symmetry along the z direction, and furthermore, if the lattice vibrations are temporarily neglected, the spacing between the states with quantum numbers m_z and $m_z - 1$ is given by

$$h\nu_0 = (ehQ/2I(2I - 1))(\partial^2 V/\partial z^2)(3m_z - {}^3/_2) \qquad (2\text{-}2)$$

Thus the level spacings are proportional to the product of the nuclear quadrupole moment Q and the principle value $\phi_{zz} = \partial^2 V/\partial z^2 = q_0$ of the field gradient tensor. Transitions between these levels may be induced by the interaction between the nuclear magnetic moment and an applied radio frequency magnetic field. A measurement of pure quadrupole resonance frequency thus provides information on the electric field gradient at the nuclear position in the solid.

It is obvious that the application of hydrostatic pressure will alter the field gradients at the nucleus by changing the interatomic separations in the solid. Thus by 1955 a number of workers (43–47) had observed the effect of hydrostatic compression on the pure quadrupole resonance frequency.

In order to analyze these experiments adequately it is necessary first to include the effect of the lattice vibrations. Following the discovery of pure quadrupole resonance, Bayer (47) found that the resonance frequency ν was a strong function of the temperature, and he presented a simple theory to explain this. In the presence of lattice vibrations the components of the field gradient tensor ϕ_{ij} in a fixed coordinate system will fluctuate. This fluctuation is at a higher frequency than that corresponding to the spacing of the energy levels of the system, so that only the average value of these fluctuating components ϕ_{ij} will enter into a determination of the energy. Bayer considered a simple model of the vibration in which the field gradient tensor

components did not change in magnitude, but the tensor as a whole oscillated in an angle θ around some equilibrium direction. In such a model the value of $q_0 = (\partial^2 V/\partial z^2)$ is reduced due to the averaging process to $q_0(1 - 3\overline{\theta^2}/2)$ (assuming $\theta \ll \pi/2$). In Bayer's picture the observed decrease in ν as T increases was due to the increase in the amplitude of the thermal vibrations. The Bayer theory is successful in qualitatively explaining the observed temperature variation of ν but fails quantitatively. Kushida later generalized (48) Bayer's theory to include the effects of all the modes of vibration of the lattice and was able to show that the resonance frequency could be written as

$$\nu = \nu_0(1 - \tfrac{3}{4}\sum_i(\xi_i^{0^2}/\Theta_i)) \qquad (2\text{-}3)$$

where ξ_i^0 is the amplitude of the ith normal mode of lattice vibration and $(1/\Theta_i)$ is essentially a coefficient which describes the effect that a particular mode of vibration has on the magnitude and orientation of the field gradient tensor. For simple geometries Θ_i can be interpreted as the moment of inertia of the particular mode of motion. By recognizing that the amplitude of the ith normal mode is determined by the mean energy of the corresponding oscillator, i.e.

$$^1/_2\omega_i^2\xi_i^{0^2} = \hbar\omega_i[^1/_2 + 1/(\exp(\hbar\omega_i/kT) - 1)] \qquad (2\text{-}4)$$

it is again possible to predict the temperature variation of ν. But even Kushida's generalization of the Bayer theory was incapable of predicting the observed temperature variation quantitatively. The reason for this is that neither theory included the effect of thermal expansion on the magnitude of the components of ϕ_{ij}.

To analyze this situation somewhat more carefully, it is useful in the sum in equation (2-3) to split the lattice vibrations into low- and high-frequency terms depending whether they are above or below $\omega_M = kT_M/\hbar$, where T_M is the lowest temperature used in the experiments. The temperature variation of the

low frequency terms produces a temperature-dependence of the form (49)

$$\nu = \nu_0(1 + bT + c/T) \tag{2-5a}$$

$$b = (-3k/2) \sum_i^M (1/\Theta_i\omega_i^2) = (-3k/2)M \langle 1/\omega^2\Theta \rangle \tag{b}$$

$$c = (-\hbar^2/8k)\sum_i^M(1/\Theta_i) = (-\hbar^2/8k)M \langle 1/\Theta \rangle \tag{c}$$

Due to the appearance of the $1/\omega_i$ factor in the terms in equation (2-4), the high-frequency terms generally contribute much less than the low-frequency terms to the temperature-dependence of ν, and can often be neglected in practice. From the definition of b and c it is seen that they contain information on the vibration frequencies and effective moments of inertia of the various vibration modes of the molecules in the crystal. ν_0 contains information as to the magnitude of the principal axis of the field gradient tensor $\partial^2 V/\partial z^2$. The failure of previous attempts to fit equation (2-5a) to the experimental data was that ν_0, b, and c were considered independent of volume, that is, that they were constants independent of the volume of the solid. In fact, of course, they are not. One can estimate roughly using $(\delta\nu_0/\nu_0) \sim (\delta V/V)$ that between $0 < T < 300$ °K the frequency should change $\sim 2\%$ due to the volume effect alone. Also if ν_0, b, and c were independent of volume, the pressure-dependence of the resonance frequency would be zero. Actually, though, looking at Figure 5, which shows measurements of ν vs. pressure for Cu_2O (49), we see that this is far from being the case. To apply the theory of Kushida correctly to the experimental data it is necessary (49) to plot ν vs. volume isotherms for a range of temperatures. It is presumed that V as a function of P for various temperatures is known. Then at each volume ν_0, b, and c can be determined. To check whether the temperature variation at $P = 0$ can be explained one must determine the volume at each temperature for which $P = 0$ and put into equation (2-5a) the corresponding values of ν_0, b, and c. If this proce-

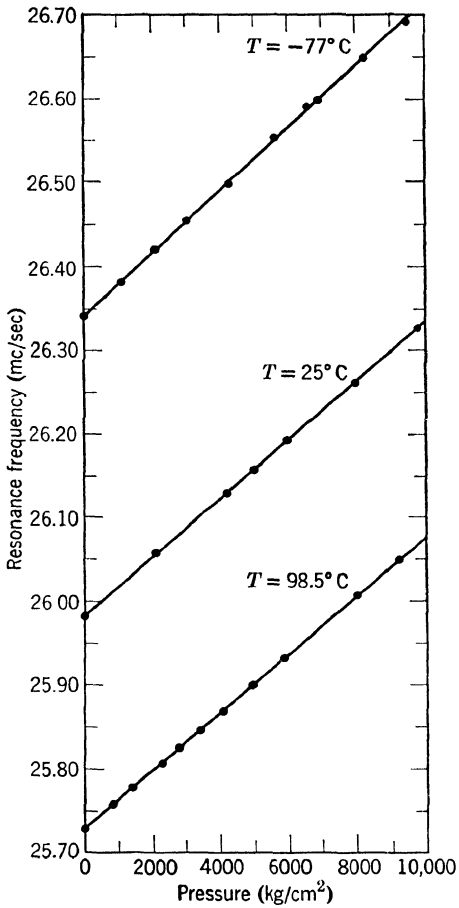

Figure 5. The pure quadrupole resonance frequency of the Cu^{63} nucleus in Cu_2O as a function of pressure for three temperatures.

dure is carried out it is possible to explain the temperature variation of the resonance frequency quantitatively.

But notice that here we have also obtained the volume-dependence of the internal field gradients from $\nu_0(V)$. Also from

$b(V)$ and $c(V)$ we have the volume-dependence of the vibration frequencies and their magnitudes. This is rather detailed information which casts considerable light on the internal electric fields and the lattice vibrations.

The analysis described above has been carried out (49) for 3 solids, Cu_2O, $KClO_3$, and *para*-dichlorobenzene, in experiments to 10,000 atm using temperatures as low as $-77°$ C and as high as 100° C. The Cu^{63} nucleus was observed in Cu_2O, the Cl^{35} nucleus was studied as $KClO_3$ and p-$C_6H_4Cl_2$.

In Cu_2O it was found that ν_0 varies with volume roughly as $(1/V)$(where $\nu(V) = \nu_0(V/V_0)^{-.96+.04}$). This is precisely what one would expect if the neighbors set up a Coulomb $(1/r^2)$ electric field at the nucleus, for in such a case

$$q_0 \propto \frac{\partial}{\partial r}\left(\frac{1}{r^2}\right) \propto \frac{1}{V}$$

This fact confirms the belief that Cu_2O is an ionic crystal. Furthermore, from the volume-dependence of b and c it was found that $\gamma = < -\partial \ln \omega_i/\partial \ln V >$ is negative—that is, the vibration frequencies decrease with decreasing volume. This result is not too surprising when it is remembered that the thermal expansion coefficient for Cu_2O is negative in certain temperature ranges, thus suggesting a negative Gruneisen's constant for certain normal modes of vibration. In $KClO_3$ q_0 changes from a $(V/V_0)^{-.022}$-dependence at $(V/V_0) = .98$ to $(V/V_0)^{-.028}$ at $1.06 = V/V_0$. In this substance the field gradient arises primarily from the ClO_3^- covalent bond, with a few percent contribution from the potassium ions. The weakness of the observed volume-dependence of q_0 is consistent with the view that the compression of the crystal changes the K^+ and ClO_3^- distances without appreciably affecting the dimensions of the ClO_3^- group. In $KClO_3$ γ has the reasonable value of about 1.8 (1.4 at $V/V_0 = .98$ and 2.2 at $V/V_0 = 1.06$). The experimental results on *para*-dichlorobenzene are so unusual that they are given in Figures 6, 7, and 8. In the same specimen these data

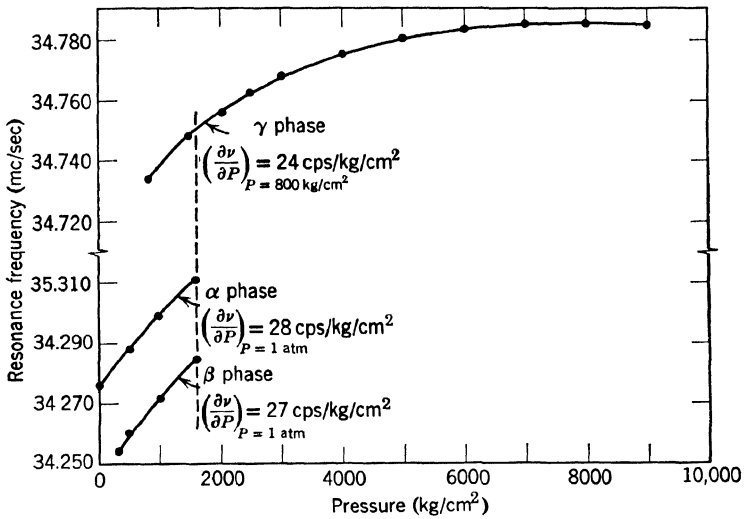

Figure 6. The pure quadrupole resonance frequency of the Cl^{35} nucleus in *para*-dichlorobenzene as a function of pressure at $T = 24.8°C$. The α, β, and γ phases are polymorphic modifications which are produced by hydrostatic pressure.

contain two phenomena dear to the heart of the high-pressure physicist: the presence of polymorphic transitions, and a maximum in the ν vs. pressure curve. At room temperature and atmospheric pressure the α phase is observed, its frequency increasing with pressure until at 1600 kg/cm^2 the line quickly disappeared. The line could be found again 436 kc/sec higher with an intensity and line width about the same as the α phase. This new phase can be identified as a γ phase (50). On increasing the pressure the ν vs. pressure curve flattens until at 8500 kg/cm^2 there is a suggestion that $d\nu/dP$ may become negative. On decreasing the pressure the γ phase can be followed below 1600 kg/cm^2 until at about 750 kg/cm^2 it disappears, to reappear once again in a β phase (50) 27 kc/sec below the α phase. The β phase is metastable relative to the α phase at room temperature, returning to it in a time which is very sensitive to the

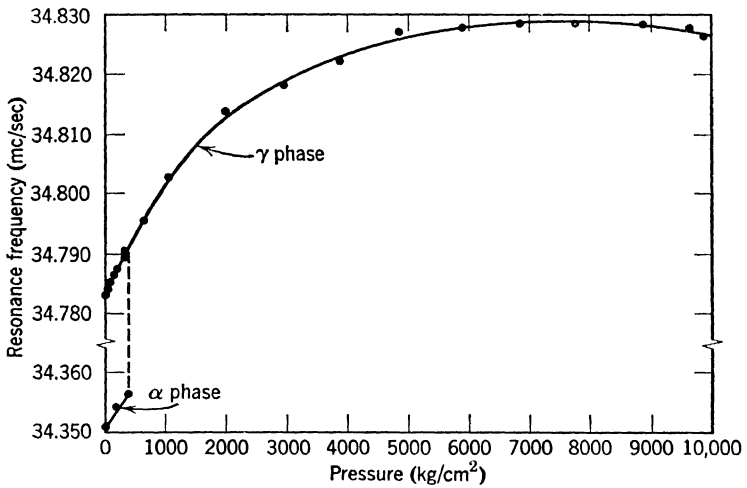

Figure 7. The pure quadrupole resonance frequency of the Cl^{35} nucleus in *para*-dichlorobenzene as a function of pressure at T = 0°C.

pressure (49). At lower temperatures we observe very clearly that the γ-phase ν vs. pressure curve does possess a maximum. The maximum which we have observed in the γ phase can be understood as follows: With a decrease in volume, the amplitude of vibration decreases, that is $\overline{\theta^2}$ decreases, thus tending to produce an increase on the resonance frequency. On the other hand, at low pressures ν_0 is roughly independent of volume. This is because the field gradient at the Cl^{35} nucleus is produced by the C-Cl covalent bonding. Since in the 0th approximation, the application of pressure to a molecular crystal changes only the intermolecular distances, q_0 can be expected to be independent of volume at the lowest pressures. However, as the volume gets smaller, the covalent bonding decreases by intermolecular hybridization with neighboring molecules. This reduces the field gradient, thereby tending to *reduce* the resonance frequency. The competition between these two effects causes the maximum in ν. The maximum shifts to lower pressures as the temperature is dropped because $\overline{\theta^2}$ starts small at low tempera-

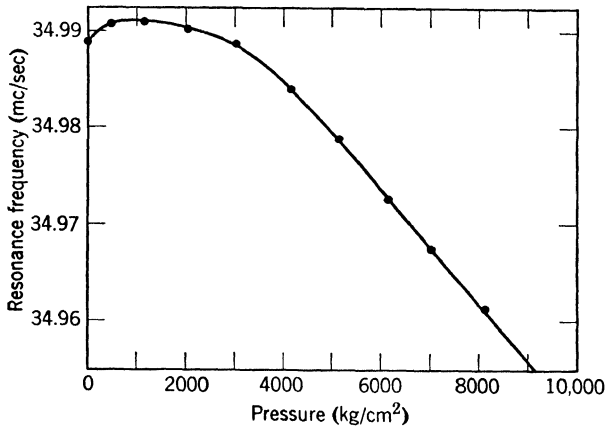

Figure 8. The pure quadrupole resonance frequency of the Cl^{35} nucleus in the γ phase of *para*-dichlorobenzene as a function of pressure at $-77°C$.

tures and it is therefore easier to overcome. Quantitatively, it is observed that at $(V/V_0) = 1.04\, q_0$ varies as V^0, while at $(V/V_0) = 0.94\, q_0$ varies as $V^{0.035}$. γ is about 1 and is roughly independent of volume.

Recently T. Fuke, working in Professor Koi's laboratory at Tokushima University, has observed (51) the pure quadrupole resonance spectra of the I^{127} nucleus in SnI_4 and the Br^{81} nucleus in p-$C_6H_4Br_2$ under pressure up to 10,000 kg/cm². In both these crystals Fuke found results quite similar to those mentioned above for p-$C_6H_4Cl_2$. The bromine and iodine resonances occur at about 200 mc and 116 mc respectively. Nevertheless he found it possible to simply adapt the conical electrical lead for operation in this frequency region. Fuke also found that petroleum either could be used as a pressure-transmitting medium to about 1,000 kg/cm² at liquid-oxygen temperatures! This result, combined with the previous observation (49) that a 50-50 mixture of *n*-pentane and 2-methylbutane will not freeze below 10,000 kg/cm² at 196° K, means that a high-pressure press designed to use a liquid pressure-transmitting medium can be used effectively as low in temperature as 90° K. Fuke

also studied the As^{75} resonance in As_5O_6 and the Br^{81} resonance in $KBrO_3$, and analyzed all his results along the lines described above.

The negative slopes ($d\nu/dP$) which we have noted for the γ phase in p-$C_6H_4Cl_2$ are about ten times smaller than those observed for the Cl^{35} resonance in $HgCl_2$ (52) and the Br^{81} resonance in $TiBr_4$ (53). In this latter compound, Barnes and Engardt (53) have concluded that this negative pressure-dependence of the quadrupole resonance frequency can explain the strange temperature-dependence of the resonance frequency. In $TiBr_4$ the resonance frequency *increases* with increasing temperature from $-250°$ C to $-50°$ C, until at this temperature it starts to behave normally and decreases with increasing temperature. They argue that the thermal expansion causes the resonance frequency to increase as the temperature is raised, because $(d\nu/dV) = (d\nu/dP)(dP/dV) > 0$. This product is positive because both $d\nu/dP$ and dP/dV are negative. However, the lattice vibrations tend to *lower* the resonance frequency. This effect dominates above $-50°$ C, while below this temperature the thermal expansion effect dominates.

By measuring the pressure-dependence of the quadrupole splitting of the nuclear magnetic resonance lines of Na^{23} in $NaClO_3$ and $NaBrO_3$, Gutowsky and Williams (54) were able to show that the electric field gradient at the sodium nuclei varies approximately as V^{-2}. It was pointed out in this work, and in a later study of $NaNO_3$ (55), that in order to analyze this result it was important to keep in mind that the distortions in the unit cell will not in general be specified by a single parameter, V, the volume of the unit cell, even though the compression is hydrostatic. They realized that in order to calculate theoretically the pressure-dependence of field gradient it is necessary to know how the pressure affects the internal parameters which describe the position of each of the atoms within the unit cell. This point was also made by W. M. Walsh (56) in his study of the effect of pressure on the crystalline field splitting of the ground state of Ni^{2+} in $NiS_6F_6 \cdot H_2O$. These observations made it clear that con-

comitant measurements of the pressure-dependence of the x-ray structure factors may make a valuable contribution to studies of the pressure-dependence of the pure quadrupole spectra.

The effect of pressure on the quadrupole resonance in a metal has been studied in the case of gallium (57). Despite the complexity of the crystal structure of this metal, unpublished analysis of the data indicates that the field gradient at the gallium nucleus varies roughly as $1/V$.

2.2 Higher Moments of the Crystalline Fields

When a free ion is substituted into a crystalline lattice, its electrons experience the electrostatic field set up by the neighboring ions in the lattice. The angular and radial dependence of the electrostatic potential which the central ion experiences can be described in terms of an expansion in powers of the quantity $\mathbf{r}/R$, where $\mathbf{r} = \hat{\imath}_x x + \hat{\imath}_y y + \hat{\imath}_z z$ is the distance from the central ion to the point at which the potential is evaluated, and R is the distance between the central ion and the nearest-neighbor ions. In the case that the neighbor ions are arranged on the 6 corners of an octahedron around the central ion, the lowest nonvanishing terms in the expansion of the potential apart from the spherically symmetrical term is

$$V_{\text{octahedral}} = D(x^4 + y^4 + z^4 - 3r^4/5) + O(r^6/R^7) + \ldots \quad (2\text{-}6)$$

D is a coefficient which depends on R and the detailed charge distribution of the neighbors. If the neighbors are regarded as points with charge ze then

$$D = (35/4)\ (ze/R^5) \quad (2\text{–}7)$$

It will be remembered that a similar expansion of the electric field occurs in the case of the interaction between the nuclear quadrupole moment and the crystalline electric field. However in that case the most important terms in the expansion are those corresponding to derivatives of the form $(\partial^2 V/\partial r^2)_{r=0}$. In the

case of point charges this leads to quadrupole coupling constants which vary with R as $1/R^3$. In the paramagnetic resonance case the important quantity is the dependence of D, or $(\partial V^4/\partial r^4)_{r=0}$, on R. The simple point charge approximation equation (2-7) leads then to a $1/R^5$ dependence for this quantity.

As a result of this crystalline potential (equation (2-6)), the spatial degeneracy of the orbital states of the free ion is lifted, i.e. the atomic term values are split. If the degeneracy of the ground state is completely removed by the crystalline field, the orbital angular momentum will be quenched, i.e. the expectation value of any component of **L** will be zero. Thus as far as the magnetic properties of the ion are concerned the orbital contribution to the magnetic moment in first order will be zero. Physically what occurs is that the crystalline field exerts torques on the orbit of the electrons which continuously reorient the plane of rotation. As a result, on the average the orbital contribution to the magnetic moment is zero. Thus in first approximation one would expect that the interaction between the ion and an external magnetic field would be described solely by the spin Hamiltonian

$$\mathcal{H} \cong g_0 \beta \mathbf{H} \cdot \mathbf{S} \tag{2-8}$$

where $g_0 = 2.0023$. A paramagnetic resonance investigation of the energy levels of this Hamiltonian would yield only g_0. However, in the next highest approximation it is easy to see that the application of a magnetic field slightly "unquenches" the orbital angular momentum through the spin orbit coupling. Physically, the application of the magnetic field orients the spin moment; the spin moment in turn is coupled to the orbital moment via the spin orbit interaction $\lambda \mathbf{L} \cdot \mathbf{S}$. Thus the oriented spin will partly orient the orbital moment. According to second-order perturbation theory (58) the magnitude of the orbital contribution $\beta \langle L \rangle$ can be expected to be the order of $\beta(\lambda/\Delta)$, where λ is the spin orbit coupling constant and Δ is the crystalline field splitting of the orbital levels. As a result of this effect the magnitude of the g value in the spin Hamiltonian will depart from

2.0023, and in general will depend upon the direction of the magnetic field relative to the crystalline axes. The deviation of g from g_0 provides information jointly about the spin orbit coupling constant and the crystalline field splitting of the free-ion states.

W. M. Walsh (36) has taken advantage of this fact to use the paramagnetic resonance method to study the effect of pressure on the crystalline field splitting. He studied the ions Ni^{2+} and Cr^{3+} substituted into the cubic crystal MgO. In this crystal the impurity ion is surrounded by a nearest-neighbor octahedron of O^{2-} ions. Both Ni^{2+} and Cr^{3+} are in orbital F states in the free ion, the spin being $S = 3/2$ for Cr^{3+} and $S = 1$ for Ni^{2+}. The octahedral crystalline field splits the orbital F states into two triplets and a singlet, the singlet lying lowest. Denoting the singlet-triplet splitting by Δ, and using the point charge approximation for the potential (equations (2-6) and (2-7)), it follows that Δ is given by

$$\Delta = (10/3)(e^2\langle r^4\rangle/R^5) \tag{2-9}$$

where $\langle r^4\rangle$ is the average value of r^4 for electrons in $3d$-orbitals on the metal ion. Because of the cubic symmetry of the crystal field, the g value is isotropic and the spin Hamiltonian is

$$\mathcal{H} = g\beta\mathbf{S}\cdot\mathbf{H} \tag{2-10a}$$

where

$$g = g_0(1 - (4\lambda/\Delta)) \tag{b}$$

By observing the paramagnetic resonance spectrum under hydrostatic pressure, Walsh found (36) that for Cr^{2+} in MgO g changes from 1.97970 ± 0.00003 to 1.97995 ± 0.00003 as the pressure changes from 1 to 10,000 kg/cm^2 (see Figure 9). This result demonstrates clearly the precision required in these experiments. The high accuracy was achieved by means of a feedback loop from the output of the paramagnetic resonance spectrometer to the current control on the magnet. Using this loop the magnetic field was locked to the center of the resonance line.

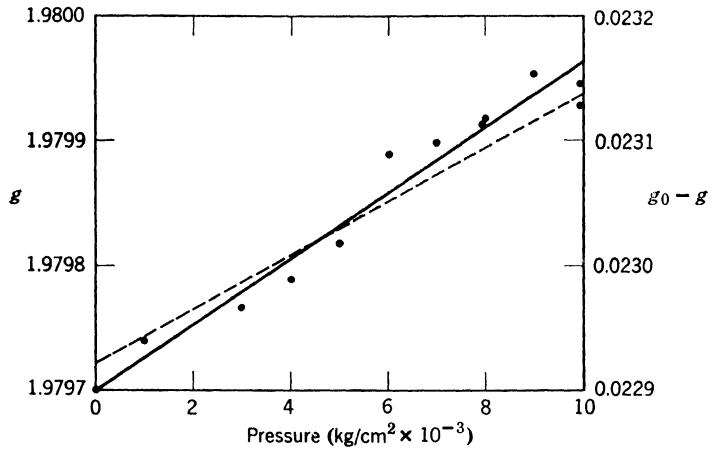

Figure 9. The pressure-dependence of the g-value for the paramagnetic resonance spectrum of Cr^{3+} in MgO.

Any shifts in the magnetic field corresponding to the center of the line could be determined using a nuclear resonance probe to a few parts in 10^5. Walsh found that

$$1/(g - g_0)(d(g - g_0)/dP)_T = \begin{matrix} 1.14 \times 10^{-6}/(\text{kg/cm}^2) & Cr^{3+} \text{ in MgO} \\ 1.08 \times 10^{-6}/(\text{kg/cm}^2) & Ni^{2+} \text{ in MgO} \end{matrix} \quad (2\text{-}11)$$

In order to transform this into a form which shows the dependence of $(g - g_0)$ on the distance between the metal ion and the oxygen neighbors one must know the compressibility in the neighborhood of the metal ion. In the case of Ni^{2+} it is reasonable to use the compressibility of bulk MgO, since NiO and MgO have nearly identical lattice constants. While this is not the case for Cr^{3+} ion, the compressibility of MgO was used there too to determine the dependence of (λ/Δ) on R. Walsh found

$$d \ln (g - g_0)/d \ln R = \begin{matrix} (6.0 \pm 0.6) & \text{for } Cr^{3+} \text{ in MgO} \\ (5.7 \pm 0.9) & \text{for } Ni^{2+} \text{ in MgO} \end{matrix} \quad (2\text{-}12)$$

If we look back at equations (2-9) and (2-10), and if λ and $\langle r^4 \rangle$ are regarded as independent of R, we find at once that

$$\partial \ln (g - g_0)/\partial \ln R = -\partial \ln \Delta/\partial \ln R = +5.0 \quad (2\text{-}13)$$

Thus, within the restrictions imposed by the assumptions made above, the simple point-charge picture seems nearly capable of accounting for the observed dependence of the orbital moment on the interatomic distances. However, an examination (36) of the *magnitude* of λ/Δ indicates that the point-charge picture is incapable of yielding the observed *magnitude* of $(g - g_0)$.

In case the free ion has zero orbital angular momentum in its ground state (e.g., Mn^{2+} and Fe^{3+}) one would think that there would be no interaction between the spin and the crystalline electric field. However, such an interaction, while small, can be observed in the paramagnetic resonance spectra of these S-state ions (59) in MgO. If one also includes the effect of the hyperfine interaction $(A\mathbf{I}\cdot S)$ between nuclei and electrons, the spin Hamiltonian describing the spectrum is given by (36)

$$\mathcal{H} = g\beta \mathbf{H}\cdot \mathbf{S} + (1/6)a(S_x^4 + S_y^4 + S_z^4) + A\mathbf{I}\cdot \mathbf{S} \quad (2\text{-}14)$$

in which g is very close to the free-electron value. The term of present interest is the second on the right hand side of equation (2-14) whose magnitude is given by a, the so-called ground-state splitting parameter. A detailed mechanism for this coupling between the spin and the crystal field is not yet clearly established (60,61), and a physical description of the proposed mechanism is difficult as the calculation involves simultaneous inclusion of the spin orbit, magnetic spin-spin and crystal field interactions, carried out to the sixth order of perturbation theory. Different predictions (60,61) have been made for the dependence of a on the interatomic distances. Watanabe finds (60) $a\alpha(Dq)^2$, i.e. $(\partial \ln a/\partial \ln R) = -10$ if the point-charge model is used. On the other hand, Powell, Gabriel, and Johnston (61) have calculated the dependence of a on the crystalline field splitting parameter Dq where $q = 4e\langle r^4 \rangle/105$ and D is given in the point-charge model by equation (2-7). They find $(\partial \ln a/\partial \ln Dq) = 2.1$ and

3.5 respectively for Mn^{2+} in ZnS and MgO. If we use Walsh's results described above for Cr^{3+} and Ni^{2+} in MgO to estimate the dependence of Dq on R for *both* ZnS and MgO we find $\partial \ln Dq/\partial \ln R = -6$. (This procedure is clearly questionable in the ZnS case.) One is led, using Powell, Gabriel, and Johnston's calculation for $\partial \ln a/\partial \ln Dq$ to

$$(\partial \ln a/\partial \ln R)_{\text{theor}} = \begin{matrix} -12 & Mn^{2+} \text{ in ZnS} \\ -21 & Mn^{2+} \text{ in MgO} \end{matrix} \quad (2\text{-}15)$$

Walsh has also measured (36) the paramagnetic resonance spectra of Mn^{2+} in ZnS and MgO as a function of pressure and has determined the pressure-dependence of the ground-state splitting parameter. Assuming that the local compressibility is identical to that of the host lattice, Walsh found

$$(\partial \ln a/\partial \ln R)_{\text{expt}} = \begin{matrix} -9.6 & Mn^{2+} \text{ in ZnS} \\ -21.2 & Mn^{2+} \text{ in MgO} \end{matrix} \quad (2\text{-}16)$$

which supports the Powell-Gabriel-Johnston calculation. As this discussion shows, these high-pressure measurements are very useful in establishing the correct theoretical description of such a subtle quantity as the ground-state splitting parameter of these S-state ions.

2.3 The Isomer Shift

The work of R. Mossbauer (62) has shown that an appreciable fraction of the γ-rays emitted by nuclei bound in solids are emitted without recoil of the parent nucleus. The solid as a whole may take up the recoil momentum, provided that the emitted γ-ray energy is not too large. Since the lifetime (τ) for emission for the γ-ray can be quite long, the energy of the emitted γ-ray can be extremely well defined. For example, in the case of the decay of Fe^{57} from its excited $I = {}^3/_2$ state to the $I = {}^1/_2$ ground state $\tau \sim 1.4 \times 10^{-7}$, hence the uncertainty in γ-ray energy $\hbar/\tau$ divided by the γ-ray energy $E = 14.4$ kev is $\Delta E/E = 4 \times 10^{-13}$. The difference in γ-ray energy between nuclei in a source and an absorber can be observed by detecting

the resonant absorption of γ-rays by an absorbing foil. The resonance curve can be swept out by changing the velocity of the source relative to that of the absorber (63). In this way the Doppler shift is used to sweep the energy of the γ-ray.

Using this method it has been found that the energy of the γ-ray depends not only on the spacing of the energy levels of the bare, static nucleus, but also upon (*a*) the electrostatic interaction between the nuclear charges and the electronic charge inside the nucleus (64,65,66): the isomer shift, (*b*) the magnetic hyperfine interaction between the nucleus and its surrounding electrons (67), (*c*) the quadrupole interaction between the nucleus and the crystalline electric field gradients, and (*d*) the temperature. This last dependence comes about through the time dilatation produced in second order by the vibration of the nuclei about their equilibrium positions (68).

The Mossbauer effect has proven to be a most useful tool for the study of solids because the γ-ray energy carries with it information on the electronic structure and atomic motion in the solid. Furthermore, the sharpness of the γ-ray emission line enables a measurement of exceptionally small changes in the energy of the γ-ray. In fact, R. Pound, G. Benedek, and R. Drever (69) have measured the effect of hydrostatic pressure on the energy of the 14.4-kev γ-ray from ferromagnetic iron. The γ-rays emerge from the high-pressure vessel through a conical beryllium window. While this experiment is not a magnetic resonance experiment, it provides information so like that which we have discussed previously that it seems appropriate to include it.

Since ferromagnetic iron is cubic, the quadrupole interaction in the $I = {}^3/_2$ state is absent. Furthermore, the method of observing the spectrum is to superpose the hyperfine pattern in the source over that in the absorber so that in fact one detects changes in the center of gravity of the hyperfine pattern of the source. Thus, changes in the energy of the γ-ray come solely from changes in the quantity:

$$h\nu = h\nu_0 + h\nu_{\text{isom}} + h\nu_{\text{rel}} \qquad (2\text{-}17)$$

The term $h\nu_0$ represents the spacing of the energy levels of a stationary nucleus free of encircling electrons and external electric and magnetic fields. The $h\nu_{\text{isom}}$ represents the electrostatic interaction between the nuclear charge and the electronic charge density inside the nucleus. This interaction depends on the effective nuclear radius, so that if this radius is different in the excited and ground states there will be a change in the electrostatic interaction energy which appears in the energy of the γ-ray. To get some feeling for this effect one may consider a spherical uniformly charged nucleus (charge Ze) interacting with the electronic charge density at the nucleus $e|\psi(0)|^2$. The difference in energy between the excited and ground state is

$$h\nu_{\text{isom}} = (2/5)\pi Ze^2(\rho^2_{\text{ex}} - \rho^2_{\text{gr}})|\psi(0)|^2$$

where ρ_{ex} and ρ_{gr} are the radii of the excited and ground states respectively. Of course in general we have

$$h\nu_{\text{isom}} = K|\psi(0)|^2$$

where the constant K can be evaluated (66) by observing the difference in isomer shifts between iron atoms in different degrees of ionization. If one then employs the free-ion wave functions (70) to calculate the difference in $|\psi(0)|^2$, K can be found. The size of $h\nu_{\text{isom}}$ relative to $h\nu_0$ is as follows: The core electron contribution (66) in iron is $(\nu_{\text{isom}}/\nu_0)_{\text{core}} = -2 \times 10^{-8}$; the outermost $4s$ electrons give $(\nu_{\text{isom}}/\nu_0) = -5 \times 10^{-12}$. The minus sign comes from the fact that the "radius" of the excited state in iron is smaller than the ground state (66). While these are very small contributions, it should be kept in mind that the γ-ray emission line is extremely narrow; our estimate above shows $\Delta E/E \sim 4 \times 10^{-13}$.

The relativistic contribution due to the time dilatation produced by the oscillation of the Fe^{57} atom about its equilibrium lattice position is calculated as follows:

$$\nu_{\text{rel}} = \nu_0(1 - \langle v^2\rangle/c^2)^{1/2} - \nu_0 \qquad \text{(2-18a)}$$

$$\cong -\nu_0(M\langle v^2\rangle/2Mc^2) \qquad \text{(b)}$$

$$\cong \nu_0(\bar{E}/2Mc^2) \qquad \text{(c)}$$

where M is the mass of the atom, and $\bar{E}$ is the average vibrational energy of an iron atom. The size of ν_{rel} in terms of ν_0 is $(\nu_{rel}/\nu_0) = -7 \times 10^{-13}$.

By making measurements at 1, 2000, and 3000 kg/cm^2 the pressure coefficient of the γ-ray energy was found to be (69)

$$(1/\nu)(\partial\nu/\partial P)_T = -(2.61 \pm 0.01) \times 10^{-18}/(\text{kg/cm}^2) \quad (2\text{-}19)$$

Thus on applying 3000 kg/cm^2, our maximum pressure, the γ-ray energy changed only 7.8 parts in 10^{15}! This is by far the smallest effect ever measured under high pressure. The γ-ray energy changes under pressure through two effects. The first is the change produced in $|\psi(0)|^2$ by altering the volume of the unit cell; the second is the change in the Debye temperature, which in turn alters the average vibrational energy $\bar{E}$. An estimate of the latter effect can be made. Using the common assumption (71) that $(\partial \ln \Theta/\partial \ln V) \cong -\gamma$, where γ is Gruneisen's constant, one finds at 295° K that the effect of pressure on the relativistic term is (69) $\sim -.126 \times 10^{-18}/(\text{kg/cm}^2)$ which is less than 5% of the measured pressure coefficient given in equation (2-19). Thus the volume-dependence of the isomer shift must be responsible for the observed pressure coefficient, i.e.

$$(1/\nu)(\partial\nu/\partial P)_T \cong (K/\nu)(\partial|\psi(0)|^2/\partial \ln V)(\partial \ln V/\partial P) \quad (2\text{-}19)$$

Using a value of K obtained as described previously, along with Bridgman's value (72) for the compressibility of iron, we find, using atomic units (1 a.u. = 0.5292×10^{-8} cm),

$$(\partial|\psi(0)|^2/\partial \ln V) = -(2.7 \pm 0.4) \text{ a.u.}^{-3} \quad (2\text{-}20)$$

We may combine the present result with that discussed previously (Section 1.4) in the case of nuclear resonance in iron. In that experiment one obtains the volume-dependence of the difference between spin-up and spin-down charge densities. Using Kouvel's data for the pressure-dependence of the magnetization, one finds

$$\frac{1}{|\psi_\uparrow(0)|^2 - |\psi_\downarrow(0)|^2} \frac{\partial(|\psi_\uparrow(0)|^2 - |\psi_\downarrow(0)|^2)}{\partial \ln V} = -0.19 \quad (2\text{-}21)$$

From the magnitude and direction of the magnetic field at the nucleus one may deduce that

$$|\psi_\uparrow(0)|^2 - |\psi_\downarrow(0)|^2 = 0.63 \text{ a.u.}^{-3} \tag{2-22}$$

Thus

$$\frac{\partial(|\psi_\uparrow(0)|^2 - |\psi_\downarrow(0)|^2)}{\partial \ln V} = -0.12 \text{ a.u.}^{-3} \tag{2-23}$$

while equation (2-20) gives

$$\frac{\partial|\psi_\uparrow(0)|^2 + |\psi_\downarrow(0)|^2}{\partial \ln V} = -(2.7 \pm 0.4) \text{ a.u.}^{-3} \tag{2-24}$$

Note that $\uparrow$ denotes a spin in the same direction as the magnetization of the solid. From equations (2-24) and (2-23) we may conclude that on changing the volume of the unit cell, the major effect consists in changing both the spin-up and spin-down charge densities by about the same amount, namely $\partial|\psi_\uparrow(0)|^2/\partial \ln V \sim \partial|\psi_\downarrow(0)|^2/\partial \ln V \sim -1.3$ a.u.$^{-3}$. However, the spin-up charge density at the nucleus changes slightly more strongly than the spin-down density. Quite apart from the individual volume-dependences of the spin-up and spin-down charge densities, we may estimate the magnitude of the volume-dependence of the total charge density at the nucleus in the following way. If we assume that only the 4*s* wave function $|\psi_{4s}(0)|^2$ is changed by the volume compression, and that $|\psi_{4s}(r)|^2$ scales with the volume, i.e., $(\partial \ln |\psi_{4s}(0)|^2/\partial \ln V) = -1$, then the estimate (66) that $|\psi_{4s}(0)|^2 \approx 3$ a.u.$^{-3}$ gives $(\partial|\psi(0)|^2/\partial \ln V)_{\text{estimate}} = -3$ a.u.$^{-3}$. This estimate compares favorably with the experimental result in equation (2–20). These results show that the combined techniques of nuclear magnetic resonance, the Mossbauer effect, and high-pressure physics can provide very detailed information concerning the electronic structure in iron.

3. Relaxation, Diffusion and Hindered Rotation in Solids

3.1 Nuclear Relaxation in the Alkali Metals

We have considered previously the information which can be obtained from precise measurements of the frequency positions

of absorption lines in the magnetic resonance spectra. Considerable information, however, is contained in measurements of the line shapes and relaxation times. These quantities can provide rather detailed information on atomic and molecular motion in solids.

The work of D. Holcomb and R. E. Norberg (73) is a fine example of the use of nuclear magnetic resonance at atmospheric pressure as a tool for the study of atomic diffusion in solids. These workers measured the temperature-dependence of the nuclear relaxation times of the alkali metals (lithium, sodium, and rubidium) over a wide range of temperature. By careful analysis of their data they determined the magnitude and temperature-dependence of the self diffusion coefficient D for lithium, sodium, and rubidium.

The self diffusion coefficient, D, may be defined in terms of the partial differential equation which governs diffusion. If $P(r, t)$ is the probability that a diffusing particle may be found at time t at position r, then P is governed by the equation

$$\partial P/\partial t = D\nabla^2 P$$

The physical significance of D may be found by considering the solution of the diffusion equation subject to the initial condition that at $t = 0$ the particle was definitely at $r = r_0$. Under these conditions P is given by

$$P(r, t) = \{1/(4\pi Dt)^{3/2}\} \exp\{-(r - r_0)^2/4Dt\}$$

From this we see that the mean square displacement of the particle increases linearly with the time as $\overline{(r - r_0)^2} = 2Dt$. The diffusion coefficient D determines the rate at which the mean square displacement increases. One can provide alternatively a microscopic description of the diffusion coefficient by turning to the microscopic random walk process which leads to the diffusion equations. This analysis shows that D is related to the mean square step length Δ^2 and the correlation time τ required for a diffusion jump by the equation

$$D = c\Delta^2/\tau$$

where c is a numerical constant of the order of 0.1 to 1.0.

Stimulated by the work of Holcomb and Norberg, R. G. Barnes, R. D. Engardt, and R. A. Hultsch (74) measured the pressure-dependence of the nuclear resonance *line width* in lithium to 3000 atmospheres, and from this estimated the pressure-dependence of the diffusion coefficient. This experiment showed that large and easily detectible changes in the nuclear relaxation times could be produced by the application of pressure to the alkali metals. As a result Hultsch and Barnes (75) undertook a detailed study of the relaxation times using the methods of spin echoes (76,77). These workers succeeded in determining the pressure-dependence of the diffusion coefficients in lithium and sodium.

The ideas on which this more complete work is based are as follows. The approach to thermal equilibrium of the nuclei can be described in terms of two relaxation times, T_1 and T_2. The spin-spin relaxation time (T_2) denotes the time required for the nuclear spins to establish thermal equilibrium between one another at some spin temperature, T_s. The quantity T_2 also characterizes the time during which phase coherence can be maintained between nuclear spins precessing in the absence of an rf field. The spin-lattice relaxation time, T_1, denotes the time required for the spin system to come to the temperature of the lattice. In simple physical terms T_1 is the time constant for the establishment of the full nuclear magnetization after applying a d.-c. magnetic field to an initially unmagnetized nuclear spin system.

Both T_1 and T_2 arise from two sources: (*1*) the nuclear dipole-dipole interaction, and (2) the hyperfine interaction between nuclei and the conduction electrons. Since the reciprocals of the relaxation times are proportional to transition probabilities, and since the transitions produced by mechanisms (*1*) and (2) are independent, it follows that

$$(1/T_1) = (1/T_1)_e + (1/T_1)_d \qquad (3\text{-}1)$$

where $(1/T_1)_e$ is the contribution from the conduction electrons, while $(1/T_1)_d$ comes from the dipolar interaction between nuclei. A similar equation holds for T_2

$$(1/T_2) = (1/T_2)_e + (1/T_2)_d \tag{3-2}$$

Since the coupling with the conduction electrons produces a field at the nucleus which fluctuates so rapidly that the "motional narrowing limit" applies (78), $T_{1_e} = T_{2_e}$. Thus, we have from equations (3-1) and (3-2) that

$$(1/T_2)_d - (1/T_1)_d = ((1/T_2) - (1/T_1)) \tag{3-3}$$

The spin-spin relaxation time, $(T_2)_d$, is itself constituted of two parts (79)

$$(1/T_2)_d = (1/T_2')_d + (1/2T_1)_d \tag{3-4}$$

where the first term on the right hand side comes from frequency components of the perturbing dipole fields near zero frequency and the second term represents a broadening due to the finite lifetime of the nuclear spin-states. Placing equation (3-4) into equation (3-3) we find that

$$(1/T_2')_d = ((1/T_2) - (1/T_1)) + (1/2T_1)_d \tag{3-5}$$

While T_1 and T_2 can be measured experimentally, $(T_2')_d$ and $(T_1)_d$ are the quantities which carry information on the diffusion constant. The theory of nuclear relaxation developed by Bloembergen, Purcell, and Pound (79) and somewhat extended to apply to diffusion in solids (73) shows that if the correlation time τ_c corresponding to a diffusion jump is small compared to the reciprocal of the rigid lattice line width $\Delta\omega$ (i.e. if $\Delta\omega\tau_c \ll 1$), then

$$(1/T_2')_d = 4\gamma_N^4\hbar^2 I(I+1)N/5Dd \tag{3-6}$$

where N = number of nuclei per unit volume, D = the self diffusion coefficient, and d = distance of closest approach of two

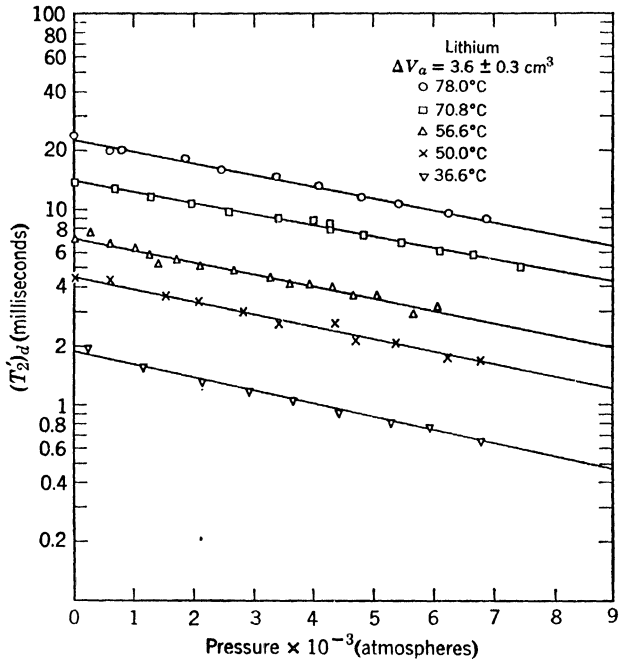

Figure 10. The dipolar relaxation time $(T_2')_d$ in lithium as a function of pressure for various temperatures. The average values of the activation volume per mole for the five temperatures is 3.6 ± 0.3 cm.[3]

nuclei. On the other hand, if ω is the Larmor frequency $(T_1)_d$ is given by

$$(1/T_1)_d = 144\pi\gamma_N^4\hbar I(I+1)ND/25\omega^2 d^5 \qquad (3\text{-}7)$$

provided that $(\omega\tau_c)^2 \gg 1$. In the motionally-narrowed limit $(\omega\tau_c)^2 \ll 1$, $(T_1)_d$ is given by

$$(1/T_1)_d = 2\pi\gamma_N^4\hbar^2 I(I+1)N/5Dd \qquad (3\text{-}8)$$

In the pressure experiments of R. A. Hultsch and R. G. Barnes (75), care was taken to operate in a temperature range in which equations (3-7) and (3-6) apply. Under these conditions

$(T_1)_d$ is large and $(1/2T_1)_d$ makes a small contribution ($\sim$1%) to $(1/T_2')_d$ in equation (3-5). Thus measurements of the pressure-dependence of T_1 and T_2 are sufficient to determine $(T_2')_d$ as a function of pressure. Using equation (3-6), this provides the pressure-dependence of the diffusion constant D.

In Figure 10 we see the results of Hultsch and Barnes for the pressure-dependence of $(T_2')_d$ in lithium to 7000 kg/cm^2. It will be noted that this quantity, and hence D, decreases by a factor of three for 7000 kg/cm^2. In sodium a pressure of 3000 kg/cm^2 changes $(T_2')_d$ and D by a factor of about six.

The diffusion coefficient, D, may be written as (80)

$$D = \mu a^2 \nu_0 \exp(-\Delta G_a/RT) \tag{3-9}$$

where μ is a constant which depends on the crystal structure, a is the lattice constant, and ν_0 is the Debye frequency which is connected to the Debye temperature Θ by $h\nu_0 = k\Theta$. ΔG_a is the Gibbs free energy of activation per mole. The pressure-dependence of D results from the effect of compression on a, ν_0 and ΔG_a. We may, in fact, relate the pressure-dependence of these quantities directly to that of $(T_2')_d$ as follows: Using equations (3-9) and (3-6) it follows that

$$\Delta G_a/RT = 6 \ln a + \ln \nu_0 - \ln (T_2')_d + \ln \text{const.} \tag{3-10}$$

The last term in equation (3-10) involves quantities that are independent of the volume of the solid. The pressure-dependence of T'_2 is thus connected with that of ΔG_a, a, and ν_0 by

$$(1/RT)(\partial \Delta G_a/\partial P)_T = 2(\partial \ln V/\partial P)_T + (\partial \ln \nu_0/\partial \ln V)(\partial \ln V/\partial P)_T - (\partial \ln (T'_2)_d/\partial P)_T \tag{3-11}$$

where we have used $a^3 = (\text{const.})(V)$. If, furthermore we use the definition of the compressibility $\beta = (-\partial \ln V/\partial P)$ and, as in the discussion of the isomer shift, use $(\partial \ln \nu_0/\partial \ln V) = -\gamma =$ Gruneisen's constant, then following Nachtrieb (81) and defining the activation volume ΔV_a as

$$\Delta V_a \equiv (\partial \Delta G_a/\partial P) \tag{3-12}$$

we find at once that the pressure-dependence of $(T'_2)_d$ may be used to provide the activation volume by

$$\Delta V_a/RT = -(\partial \ln (T'_2)_d/\partial P)_T - \beta(2 - \gamma) \qquad (3\text{-}13)$$

If the measurements of $(\partial \ln (T'_2)_d/\partial P)$ are inserted in equation (3-13), and one compares the magnitude of this quantity with that of the last two terms assuming reasonable values of γ (i.e., $\gamma = 1.0$ for Li and 1.3 for sodium) it turns out that $\beta(2 - \gamma)$ is less than 5% of $(\partial \ln (T'_2)_d/\partial P)$. Hultsch and Barnes find the activation volume to be essentially independent of temperature, with magnitudes

$$\begin{aligned} \Delta V_a &= 3.6 \pm 0.3 \text{ cm}^3 \quad \text{for lithium} \\ \Delta V_a &= 9.6 \pm 0.5 \text{ cm}^3 \quad \text{for sodium} \end{aligned} \qquad (3\text{-}14)$$

Comparing these with the molar volume V_{mol} (V_{mol} = Avogadro's number $\times$ atomic volume = $N_0\Omega$), one finds

$$\begin{aligned} \Delta V_a/V_{\text{mol}} &= 0.28 \quad \text{for lithium} \\ &= 0.41 \quad \text{for sodium} \end{aligned} \qquad (3\text{-}15)$$

Hultsch and Barnes applied their results to the "dynamical theory" of diffusion (82). This theory predicts that the activation energy for diffusion (ΔH_a) is related to the heat of fusion (ΔH_m) and the change in volume on melting ΔV_m by the relation

$$\Delta V_a = (\Delta H_m/\Delta H_a)\Delta V_m \qquad (3\text{-}16)$$

ΔH_m is determined from the temperature-dependence of the diffusion constant at atmospheric pressure. Hultsch and Barnes find this relation upheld in their work. It is worth noticing that by using equation (3-16) the activation volume may be estimated by using only data obtained at atmospheric pressure. The dynamical theory also provides a law of corresponding states, namely, that

$$\ln D\alpha(T_M/T) \qquad (3\text{-}17)$$

where T_M is the melting temperature. This relation also was found valid. Finally the results of equation (3-15) may be interpreted (75) in terms of a hard-sphere vacancy model. In this model of diffusion the activation volume may be regarded as consisting of two parts, the first being N_0 times the volume of the vacancy into which the atom moves. The second contribution is N_0 times the increase in volume of the lattice when the diffusing atom is midway in its jump onto the vacancy. This latter contribution is nearly zero for the body centered cubic alkali metals, while the former would be N_0 times one atomic volume if there were no collapsing of the neighbors inward onto the vacant site. The observation that the activation volume per atom is much less than an atomic volume suggests in this model that there is considerable "relaxation" of the neighbors onto the vacant site.

3.2 Diffusion and Hindered Rotation in Solid Hydrogen

Solid hydrogen consists of a regular lattice of molecules of H_2. Because of the Pauli exclusion principle, those hydrogen molecules whose nuclear spins are in a symmetrical spin state ($I = 1$) have antisymmetrical rotational wave function (i.e., $J = 1, 3, 5 \ldots$). Such molecules are known as orthohydrogen. On the other hand, those molecules which have an antisymmetrical nuclear spin state ($I = 0$) have even rotational wave functions ($J = 0, 2, 4 \ldots$) and are known as parahydrogen. Because of molecular rotation orthohydrogen is considerably higher in energy than parahydrogen. Nevertheless the transition from ortho to parahydrogen and vice versa is very improbable, and ordinary hydrogen may be thought of as a mixture of two distinct molecules. Since the $J = 1$ state has 3 substates, the statistical weights of the 2 species indicate that the composition in metastable equilibrium should be 75% orthohydrogen and 25% parahydrogen. The ortho-para conversion rate in the solid is 1% per hour initially and decreases with the time. Since only the ortho molecules have a net nuclear spin, these alone contribute to the nuclear resonance absorption.

Nuclear resonance studies in solid hydrogen at atmospheric pressure show the following characteristics. On increasing the temperature around 10° K the line width decreases suddenly, over a range of 1–2° K, from about 6 gauss to about 1 gauss (83). As in the case of line-narrowing in the alkali metals, which was discussed in the previous section, this effect has been explained (84,85) by the rapid self diffusion of the H_2 molecules. When the internal fields begin to fluctuate rapidly compared to the Larmor frequency, the line narrows. By measuring the temperature-dependence of the line width in the region of narrowing, the activation energy for self diffusion and the correlation times can be obtained (84,85). A second marked change in the nuclear resonance line takes place near 1.5° K (83). At this temperature, side peaks on the line appear which grow in intensity at the expense of the central peak as the temperature is lowered. This change in line shape has been explained quantitatively by F. Reif and E. M. Purcell (86). In their theory, the crystalline potential set up by the neighbor molecules splits the degeneracy of the $M_J = \pm 1, 0$ sublevels. In each of these levels the orbital angular momentum is quenched. Hence, of all the interaction terms in the Hamiltonian of the hydrogen molecule (87), only the magnetic dipole-dipole interaction between the nuclei in the molecule contributes to the line shape. The line shape itself is found by properly averaging this interaction over the nondegenerate rotational states. Finally, the intensity of the nuclear resonance line as a function of time gives information on the ortho-para conversion rate.

Clearly, all three of these characteristics of the magnetic resonance line can be expected to be functions of the intermolecular distances, and hence the pressure. Recognizing this, G. Smith and C. F. Squire studied (88) the effect of pressure on the nuclear resonance line between 1.2° K and 14° K. Their pressure range was very modest. In fact it extended only to about 250 atmospheres. Nevertheless, they observed a marked effect on the temperature at which diffusion-dominated line-narrowing occurred. They determined from their data that the

application of only 230 atmospheres changed the activation energy for diffusion from 230 cal/mole (at 1 atmosphere) to 370 cal/mole. This change in activation energy corresponds at 10° K to a 100-fold increase in the correlation time for a diffusional jump. In this low-pressure region no effect was found on the temperature at which the side peaks appeared. About the same time as Smith and Squire were carrying out their experiments, W. D. McCormick and W. Fairbank carried out similar studies up to 5000 atmospheres. A preliminary account of their work (89) indicates that the temperature at which the hindered rotation transition occurs (i.e., 1.5° K at atmospheric pressure) increases with increasing pressure. They also indicate that they searched for an effect of pressure on the ortho-para conversion rate. It seems clear that the area of experimentation opened by these workers merits further and more detailed attention.

3.3 Nuclear Relaxation in Other Solids

Proton nuclear magnetic resonance studies (90) of the proton line in 2,2-dinitropropane, $CH_3C(NO_2)_2$, have shown that between −196° C and −5° C the CH_3 group is constantly reorienting itself around one of the crystalline axes. Above −5° C, however, the hindrance presented against motion through this axis disappears and the CH_3 group undergoes general reorientation or tumbling. There is also evidence that appreciable translational diffusion takes place above −5°. Associated with the transition is a sizeable change in the volume of the solid. In the temperature range −5° C to −3° C the volume per gram takes a jump of about 0.056 cm^3/gm (91). J. J. Billings and A. W. Nolle have studied the effect of hydrostatic compression on this transition, using the sudden decrease in the line width as an indicator of the transition. They find that in the range 1 to 1000 kg/cm^2 the transition temperature is a linear function of the pressure. At 1000 kg/cm^2 the transition temperature is 12° C. By also making measurements of the thermal expansion and compressibility around the transition they were able to determine the specific volume increase at the transition as a function

of the pressure. Their results show quite clearly that the onset of general reorientation is not determined solely by the establishment of a critical minimum specific volume. They found that the transition could occur at high pressure with much smaller specific volume change than occurs at atmospheric pressure, provided only that the temperature is increased somewhat. To be more specific, they found that under 1000 kg/cm^2 a temperature of over 40° C is required to produce a specific volume change equal to that at atmospheric pressure. However the transition takes place when the temperature is increased to only 12° C. This experiment shows the usefulness of the magnetic resonance-high pressure studies combined with accurate thermal expansion and compressibility measurements in elucidating the details of phase transitions in the solid.

Another study of phase transitions under pressure using magnetic resonance is that of Goodkind and Fairbank, who studied the nuclear relaxation times in solid He^3 under pressure. They observed the effect on T_1 and T_2 of crossing the α-β phase boundary. Their experiments were conducted at 1.37° K and 2.2° K with pressures up to 120 atmospheres (92).

References

1. G. Pake, *Advances in Solid State Physics*, Vol. 2, Ed. Seitz and Turnbull, Academic Press, New York, 1956.
2. E. Fermi, *Z. Physik*, **60**, 320 (1930).
3. R. Ferrell, *Am. J. Phys.*, **28**, 484 (1960).
4. J. H. Wood and G. W. Pratt, *Phys. Rev.*, **107**, 995 (1957).
5. V. Heine, *Phys. Rev.*, **107**, 1002 (1957).
6. J. C. Slater, *Phys. Rev.*, **82**, 538 (1951).
7. M. Cohen, D. A. Goodings, and V. Heine, *Proc. Phys. Soc. (London)*, **73**, 811 (1959).
8. G. B. Benedek and T. Kushida, *Phys. Chem. Solids*, **5**, 241 (1958).

8a. T. Muto, S. Kobayashi, M. Watanabe, and H. Kozima, *Phys. Chem. Solids*, **23**, 1303 (1962).

9. W. Knight, *Advances in Solid State Physics*, Vol. 2, Ed. Seitz and Turnbull, Academic Press, New York, 1956.
10. R. T. Shumacher and C. P. Slichter, *Phys. Rev.*, **101**, 58 (1955).

11. D. Pines, *Advances in Solid State Physics*, Vol. 1, Ed. Seitz and Turnbull, Academic Press, New York, 1955.
12. H. Brooks and F. Ham, *Phys. Rev.*, **112,** 344 (1958).
13. B. R. McGarvey and H. S. Gutowsky, *J. Chem. Phys.*, **21,** 2114 (1953).
14. V. Jaccarino and R. G. Shulman, *Phys. Rev.*, **107,** 1196 (1957).
15. R. G. Shulman and V. Jaccarino, *Phys. Rev.*, **108,** 1109 (1957).
16. F. M. Johnson and A. M. Nethercot, Jr., *Phys. Rev.*, **114,** 705 (1959).
17. G. B. Benedek and T. Kushida, *Phys. Rev.*, **118,** 46 (1960).
18. P. Heller and G. B. Benedek, *Phys. Rev. Letters*, **8,** 428 (1962).
19. W. Marshall and R. N. Stuart, *Phys. Rev.*, **123,** 2048 (1961).
20. A. Mukherji and T. P. Das, *Phys. Rev.*, **111,** 1479 (1958).
21. A. J. Freeman and R. E. Watson, *Phys. Rev. Letters*, **6,** 343 (1961).
22. S. S. Hanna *et al.*, *Phys, Rev. Letters*, **4,** 177 (1960).
23. A. C. Gossard, A. M. Portis, and W. J. Sandle, *Phys. Chem. Solids*, **17,** 341 (1960).
24. C. Robert and J. M. Winter, *Compt. Rend.*, **250,** 3831 (1960).
25. W. Marshall, *Phys. Rev.*, **110,** 1280 (1958).
26. S. S. Hanna *et al.*, *Phys. Rev. Letters*, **4,** 513 (1960).
27. M. Fallot, *Ann. Phys.*, **6,** 305 (1936).
28. G. B. Benedek and J. Armstrong, *J. Appl. Phys. Suppl.*, **32,** 106S (1961).
29. J. S. Kouvel and R. H. Wilson, *J. Appl. Phys.*, **32,** 435 (1961).
30. F. Galperin, S. Larin, and A. Shishkov, *Dokl. Akad. Nauk SSSR*, **89,** 419 (1953).
31. L. Patrick, *Phys. Rev.*, **93,** 384 (1954).
32. C. Kittel, private communication, 1960.
33. E. Stoner, *Proc. Roy. Soc. (London)*, **A165,** 372 (1938).
34. T. Kushida, private communication.
35. T. Kushida, A. Silver, Y. Koi, and A. Tsujimura, *J. Appl. Phys. Suppl.*, **33,** 1079 (1962).
35a. J. D. Litster and G. B. Benedek, *J. Appl. Phys.*, **34,** 688 (1963).
36. W. M. Walsh, Jr., *Phys. Rev.*, **122,** 762 (1961).
37. L. Mattarese and C. Kikuchi, *Phys. Chem. Solids*, **1,** 117 (1956).
38. A. J. Freeman and R. E. Watson, *Phys. Rev.*, **123,** 2027 (1961).
39. L. P. Kaminow and R. V. Jones, *Phys. Rev.*, **123,** 1122 (1961).
40. J. F. Dillon, Jr., *Phys. Rev.*, **112,** 59 (1958).
41. R. L. White, *J. Appl. Phys.*, **31,** 86S (1960).
42. C. Kittel, *Phys. Rev.*, **115,** 1587 (1959).
43. D. Dautreppe and B. Dreyfus, *Compt. Rend.*, **241,** 795 (1955).
44. C. Dean and E. Lindstrand, *J. Chem. Phys.*, **24,** 1114 (1956).
45. R. Livingston, private communication, 1956.
46. T. Kushida, G. Benedek, and N. Bloembergen, *Bull. Am. Phys. Soc., Ser. II*, **1,** 11 (1956).

47. H. Bayer, *Z. Phys.*, **130,** 227 (1951).
48. T. Kushida, *J. Sci. Hiroshima Univ.*, **A19,** 327 (1955).
49. T. Kushida, G. B. Benedek, and N. Bloembergen, *Phys. Rev.*, **104,** 1364 (1956).
50. C. Dean, Thesis, Harvard University, 1952 (unpublished).
51. T. Fuke, *J. Phys. Soc. (Japan)*, **16,** 266 (1961).
52. D. Dautreppe and B. Dreyfus, *Compt. Rend.*, **242,** 766 (1956).
53. R. G. Barnes and R. G. Engardt, *J. Chem. Phys.*, **29,** 248 (1958).
54. H. S. Gutowsky and G. Williams, *Phys. Rev.*, **105,** 464 (1956).
55. R. A. Bernheim and H. S. Gutowsky, *J. Chem. Phys.*, **32,** 1072 (1960).
56. W. M. Walsh, Jr., *Phys. Rev.*, **114,** 1473 ,1959.
57. T. Kushida and G. Benedek, *Bull. Am. Phys. Soc.*, **3,** 167 (1958).
58. M. H. L. Pryce, *Nuovo Cimento, Suppl.*, **3,** VI (1957).
59. W. Low, *Phys. Rev.*, **105,** 792 (1957).
60. H. Watanabe, *Phys. Rev. Letters*, **4,** 410 (1960).
61. M. Powell, J. Gabriel, and P. Johnston, *Phys. Rev. Letters*, **5,** 145 (1960); *Proc. Roy. Soc. (London)*, **A264,** 503 (1961).
62. R. L. Mossbauer, *Z. Physik*, **151,** 124 (1958); *Naturwissenschaften*, **45,** 438 (1958); *Naturforsch.*, **14a,** 211 (1959).
63. H. Frauenfelder, *The Mossbauer Effect*, W. A. Benjamin and Co., New York, 1961.
64. I. Solomon, *Compt. Rend.*, **250,** 3828 (1960).
65. S. de Benedetti, G. Lang, and R. Ingalls, *Phys. Rev. Letters*, **6,** 60 (1961).
66. L. R. Walker, G. K. Wertheim, and V. Jaccarino, *Phys. Rev. Letters*, **6,** 98 (1961).
67. R. V. Pound and G. A. Rebka, Jr., *Phys. Rev. Letters*, **3,** 554 (1959). (See also Ref. 63.)
68. R. V. Pound and G. A. Rebka, Jr., *Phys. Rev. Letters*, **4,** 274 (1960).
69. R. V. Pound, G. B. Benedek, and R. Drever, *Phys. Rev. Letters*, **7,** 405 (1961).
70. R. E. Watson, Technical Rept. No. 12, Solid State and Molecular Theory Group, Massachusetts Institute of Technology (unpublished).
71. J. C. Slater, *Phys. Rev.*, **57,** 744 (1940).
72. *Handbook of Physical Constants*, Geological Society of America, New York, 1942.
73. D. F. Holcomb and R. E. Norberg, *Phys. Rev.*, **98,** 1074 (1954).
74. R. G. Barnes, R. D. Engardt, and R. A. Hultsch, *Phys. Rev. Letters*, **2,** 202 (1959).
75. R. A. Hultsch and R. G. Barnes, *Phys. Rev.*, **125,** 1832 (1962).
76. E. L. Hahn, *Phys. Rev.*, **80,** 580 (1950).

77. H. Y. Carr and E. M. Purcell, *Phys. Rev.*, **94,** 630 (1954).
78. D. Pines and C. P. Slichter, *Phys. Rev.*, **100,** 1014 (1955).
79. N. Bloembergen, E. M. Purcell, and R. V. Pound, *Phys. Rev.*, **73,** 679 (1948).
80. D. Lazarus, *Advances in Solid State Physics*, Vol. 10, Ed. Seitz and Turnbull, Academic Press, New York, 1960.
81. N. H. Nachtrieb, J. A. Weil, E. Catalano, and A. W. Lawson, *J. Chem. Phys.*, **20,** 1189 (1952.)
82. S. A. Rice and N. H. Nachtrieb, *J. Chem. Phys.*, **31,** 139 (1959).
83. J. Hatton and B. V. Rollin, *Proc. Roy. Soc.* (*London*), **A199,** 222 (1949).
84. B. V. Rollin and E. Watson, *Conference de Physique des Basses Temperatures*, Paris, 1955, No. 63. (Centre National de La Recherche Scientifique and UNESCO, Paris, 1956.)
85. M. Bloom, *Physica*, **23,** 767 (1957).
86. F. Reif and E. M. Purcell, *Phys. Rev.*, **91,** 631 (1953).
87. N. F. Ramsey, *Phys. Rev.*, **85,** 60 (1952).
88. G. W. Smith and C. F. Squire, *Phys. Rev.*, **111,** 188 (1958).
89. W. D. McCormick and W. M. Fairbank, *Bull. Am. Phys. Soc.* **3,** 166 (1958).
90. J. G. Powles and J. G. Gutowsky, *J. Chem. Phys.*, **21,** 1695 (1953).
91. J. J. Billings and A. W. Nolle, *J. Chem. Phys.*, **29,** 214 (1958).
92. J. M. Goodkind and W. M. Fairbank, *Phys. Rev. Letters*, **4,** 458 (1960).

Liquids and Gases at High Pressure

The study of liquids and gases under high pressure may be subdivided into two general categories. The first is a study of the shifts and splittings of the nuclear resonance line centers around the values given solely by the external magnetic field, H_0. The shifts of the nuclear resonance frequencies are known as chemical shifts. These arise partly out of the diamagnetic circulation and partly out of the paramagnetic unquenching of the orbital angular momentum (1,2). The splittings of the nuclear resonance lines are produced by an indirect nuclear-nuclear spin coupling via the electrons of the molecule. Both the shifts and splittings of the nuclear resonance lines have been used extensively (3,4) in the elucidation of molecular species. Nevertheless, few studies have been made of the effect of hydrostatic pressure on the nuclear magnetic resonance spectra of liquids and gases. In Section 2.1 of this chapter we discuss the effect of hydrostatic pressure on the chemical shifts of aqueous solutions of the octahedral cobalt complexes (5,6), and the pressure-dependence of the chemical shift of the Xe^{129} resonance in gaseous xenon (7,8).

The second category under which the material of this chapter falls is the study of the effect of pressure on the diffusion constant and relaxation time of liquids and gases. This subject has received more attention than Section 2.1, and will represent the major part of this chapter.

1. Magnetic Fields in Liquids and Gases

1.1 Chemical Shifts in Octahedral Cobalt Complexes and Xenon

Soon after the discovery of the chemical shifts (9) it was observed (10) that aqueous solutions of compounds containing cobalt complexes showed large paramagnetic chemical shifts of the Co^{59} nuclear resonance. The complexes in question consist of a Co^{3+} ion surrounded by six neighbors arranged in the form of an octahedron. Examples of such complexes are $[Co(CN)_6]^{3-}$ and $[Co(NO_2)_6]^{3-}$. A detailed analysis of the chemical shifts in these complexes was first given by Freeman, Murray, and Richards (11) and Griffith and Orgel (12). Their explanation may be outlined as follows. In the free ion Co^{3+} contains six d-electrons. According to Hunds rules this ion is in the state ^5D. The nucleus in the free ion therefore experiences a magnetic field of about 10^5 gauss from the combined effects of the spin and orbital magnetic moments of the d-electrons. However, when the ion is placed in the complex the interaction between the d-electrons on the Co^{3+} ion and the neighbor (ligand) ions produces a splitting of the degeneracy of the $5d$-orbitals on the Co^{3+} into a triplet (lowest) and a doublet. The splitting between the doublet and triplet is identical with the crystal field splitting discussed in Section 2.2 of Chapter I. When the Coulomb interaction between the six $3d$-electrons is taken into account, the doublet is split into two states labeled $^1T_{1g}$ and $^1T_{2g}$, the former being the lowest. We denote the total splitting between the ground state and the $^1T_{1g}$ state by the quantity Δ. The splitting Δ in these complexes is larger than the coupling energy responsible for the parallel alignment of the electron spins. As a result, Hunds rule breaks down and the six electrons completely fill the lower triplet, producing a state with $S^2 = 0$ and $\langle \mathbf{L} \rangle = 0$, i.e., the net spin is exactly zero, and while the magnitude of L is not zero the expectation value of any component of $\mathbf{L}$ is zero, i.e., the orbital angular momentum is quenched. The application of a magnetic field slightly un-

quenches the orbital angular momentum. The interaction between **L** and the magnetic field H admixes in a fraction $f \sim \beta H/\Delta$ of the $^1T_{1g}$ excited state into the ground state. The magnetic field set up by a single electron with orbital angular momentum $\hbar\mathbf{l}$ is

$$\mathbf{H}_l = \beta \mathbf{l}/r^3 \tag{1-1}$$

where β is the Bohr magneton: $e\hbar/2$ mc. Thus, the additional field at the nucleus produced by the unquenching action of the field H can be crudely estimated by setting $/\mathbf{l}/ \sim l_z \sim (\beta H/\Delta)$, which yields

$$\Delta H \sim \beta\langle 1/r^3\rangle_{3d}(\beta H/\Delta) \tag{1-2}$$

A rigorous calculation using Ramsey's theory (1), and taking the six electrons into account, gives

$$\Delta H/H = \sigma_p = 32\beta^2\langle 1/r^3\rangle_{3d}(1/\Delta) \tag{1-3}$$

The quantity σ_p is the paramagnetic contribution to the chemical shift. There is also a diamagnetic contribution, σ_d, produced by the Larmor circulation of the spherically symmetric part of the electron distribution, but this is about 10 times smaller for these cobalt complexes than the paramagnetic term, σ_p, whose magnitude is about 0.01. Equation (1-3) has been confirmed (11,14) by studies of σ vs. Δ, where Δ is altered by changing the nature of the ligand (e.g., replacing $Co(NH_3)_6$ by $Co(NO_2)_6$). The magnitude of Δ for each complex is measured optically, while the chemical shift $\sigma = \sigma_p + \sigma_d$ is measured using nuclear resonance. Excellent agreement with equation (1-3) is found in the sense that the quality $\langle 1/r^3\rangle$ may be taken as a constant for all the ligands studied. Also the magnitude of $\langle 1/r^3\rangle$ as determined from equation (1-3) is quite near that found (15) from paramagnetic resonance studies on the Co^{2+} ion.

The demonstration of the validity of equation (1-3) provides the experimentalist with a new method of obtaining information on the crystal field splitting, Δ. The accuracy with which changes in σ, and hence in Δ, can be detected is estimated as follows.

Since $\sigma \sim 1\%$ at a resonance frequency (ν) of 10 mc/sec, 10^5 cps out of ν are due solely to the contribution of the chemical shift. Since the line width of the resonances are ~50 cps for

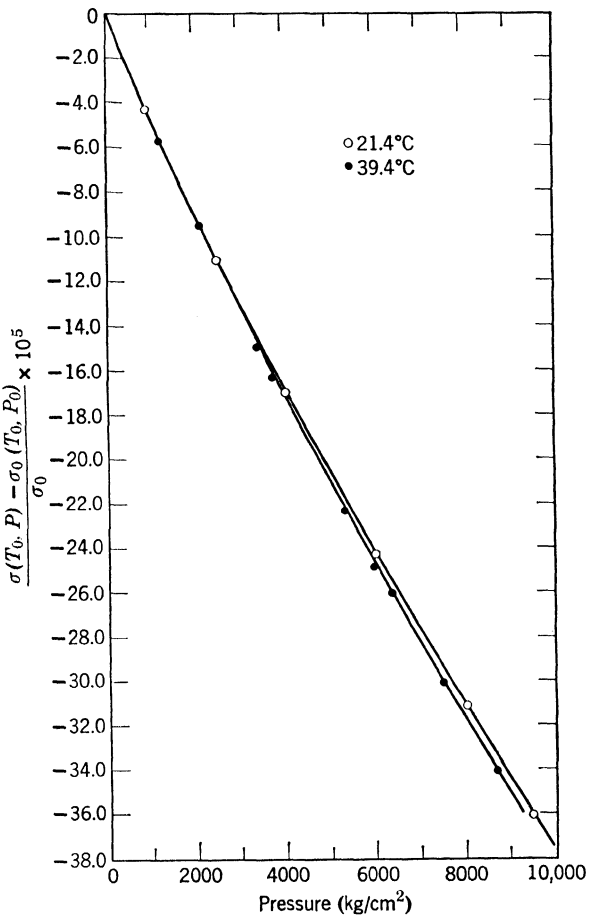

Figure 11. The change in the chemical shift $[\sigma(P_0, T_0) - \sigma(P, T_0)]$ of the Co^{59} nuclear resonance frequency in aqueous solutions of $[Co(NO_2)_6]^3$ as a function of pressure at 21.4° C and 39.4° C.

these complexes it is possible to detect a change in ν amounting to about ± 2 cps, provided that sufficient field and frequency stability of the magnet and spectrometer is provided. This sensitivity to changes in frequency corresponds to changes in σ of $\pm 2 \times 10^{-5}$. Thus, by studying the chemical shift one should be able to observe changes in Δ which are as small as a few parts in 100,000.

With these considerations in mind, an experimental study of the pressure- and temperature-dependence of the chemical shifts of the complexes $[Co(CN)_6]^{3-}$, $[Co(NO_2)_6]^{3-}$, and $[Co(NH_3)_6]^{3+}$ was undertaken (5,6). In order to achieve the stability discussed above a spectrometer-locking and magnet-control system was constructed which provided a stability of $\pm 2 \times 10^{-7}$ in both the magnetic field and the spectrometer for periods of 6 to 7 hours. An example of the results is shown in Figure 11. There we plot the pressure-dependence of σ in $[Co(NO_2)_6]^{3-}$ for 21.4° C and 39.4° C for pressures up to 10,000 kg/cm^2. In terms of frequency shifts, the Co^{59} resonance frequency changes about 3800 cps to 10,000 kg/cm,^{2} when ν_0 itself is about 10 mc. Similar data were accumulated for $[Co(CN)_6]^{3-}$ at 20.3° C, 68.5° C, and 98.1° C, and for $[Co(NH_3)_6]^{3+}$ at 19.9° C and 63.5° C. In each case it was found that $(d\sigma/dP)_{P = 1 \text{ atm}}$ was nearly independent of the temperature.

We may explain the pressure-dependence of σ by observing that the application of pressure alters the Co-ligand distance R and thereby changes Δ. In fact, one may estimate the dependence of Δ on this Co-ligand distance in the following manner. If first we regard $\langle 1/r^3 \rangle_{3d}$ as independent of R, an assumption which is consistent with the observation that $\langle 1/r^3 \rangle_{3d}$ is independent of the nature of the ligand, then turning to equation (1-3) and neglecting the small diamagnetic contribution to σ we have

$$(1/\sigma)(d\sigma/dP) \cong (1/\sigma_p)(d\sigma_p/dP) = -(1/\Delta)(d\Delta/dP) \quad (1\text{-}4)$$

For small changes in R, we may express the dependence of Δ on R as

$$\Delta = \text{constant}/R^n \quad (1\text{-}5)$$

so that equation (1-4) becomes

$$(1/\sigma)(d\sigma/dP) = n(1/R)(dR/dP) \qquad (1\text{-}6)$$

The quantity of interest is n, and its evaluation requires a knowledge of the compressibility of the complex, $(1/R)(dR/dP)$. This quantity may be estimated using the vibrational spectra of the complex. From these spectra one can obtain the force constant, k, which corresponds to the "breathing mode," i.e. the totally symmetric vibration of the complex. This force constant relates the displacement, δR, of a ligand to the force applied to each ligand in the usual normal mode treatment of molecular vibration. In the present case one may regard the applied pressure, P, as exerting a force of $PA/6$ on each of the ligands. Here A is a not too well-defined quantity that represents the effective surface area of the complex. This area may be estimated roughly by circumscribing around the ligands a sphere which just touches the atomic radii of the outermost ligand ions. With this approach one obtains

$$(1/R)(dR/dP) = -(1/R)(A/6k) = -(1/R)\ (A/6m\omega_1^2) \qquad (1\text{-}7)$$

In the last equation ω_1 is the vibration frequency of the breathing mode and m is the mass of a single ligand. One may now combine equation (1-7) with the measured values of σ and $d\sigma/dp$ to determine n from equation (1-6). The results of such a procedure are shown in Table II-1. In the next to last column we find the quantity n, which by equation (1-5) describes the R-dependence of the crystal field splitting. The last column lists the values of n which are given by the simple model that the electric field set up by the ligands can be approximated by that set up by point changes at the ligand sites. The value $n = 6$ is the result if the crystal field were produced by point electric dipoles. (The NH_3 complex is uncharged and possesses only an electric dipole moment.) The electrostatic interaction between the $3d$-electrons which in part determines the magnitude of Δ is not large enough to produce a significant difference between the distance-dependence of Δ and $10Dq$, the ligand field portion

TABLE II-1

Complex	σ	$(d\sigma/dP)$ $\times 10^3$ $(kg/cm^2)^{-1}$	R in Å	$\omega_1^2 \times 10^{-27}$ $(sec)^{-2}$	$(1/R)(dR/dP)$ $\times 10^7$ $(kg/cm^2)^{-1}$	n	n point charge model
$[Co(CN)_6]^{3-}$	0.0120	$-2.21 \pm .04$	1.83	5.86	-3.6	4.8 ± 1	5
$[Co(NO_2)_6]^{3-}$	0.0196	$-4.68 \pm .05$	2.00	6.06	-1.8	12 ± 2	5
$[Co(NH_3)_6]^{3+}$	0.0203	$-3.73 \pm .05$	2.00	11.7	-2.5	6.5 ± 1	6

of Δ. In comparing the last two columns of Table II-1 it should be borne in mind that the point-charge model is incapable of providing an adequate value for the *magnitude* of the crystal field splitting. The observed dependence on R however is consistent with this simple model at least in the case of the CN and NH_3 ligands. It may be worth reminding the reader that similar conclusions were reached in the paramagnetic resonance studies of iron-group ions in ionic crystals (See Section 2.2 of Chapter I). The crystal field splitting produced by the NO_2 ligand, however, appears to have a much stronger dependence on R than that predicted by the point charge model.

In concluding this topic it should be stressed that the method employed in determining the compressibility of the complex is a crude one. This limits the precision with which n can be established. Nevertheless, within the framework of this method it is interesting to observe that studies of the pressure-dependence of the chemical shifts of these complexes in liquids can provide much the same sort of information as do optical and paramagnetic resonance studies on solids under pressure.

A second example of measurements of the effect of pressure on the chemical shift is the work of R. Streever and H. Y. Carr (16) and E. Hunt and H. Y. Carr (17). While studying the effect of pressure on the relaxation times of Xe^{129} in xenon gas, these workers discovered that the external field, H_0, required for resonance at constant spectrometer frequency decreases as the pressure of the gas increases. They find that the change δH_0 in the field for resonance is proportional to the density of the gas and the field H_0. Their measurements taken at 25° C can be summarized by the equation

$$\delta H_0/H_0 = 4.3 \times 10^{-7}\rho \qquad (1\text{-}8)$$

where ρ is the gas density measured in amagat units. (The amagat unit is a dimensionless quantity whose magnitude is the ratio of the density of the gas at high pressure to the density at 0° C and 1 atmosphere.) This relation was obtained over a

pressure range from 30 to 110 atmospheres, which corresponds to a range of ρ from 38 to 310 amagats.

Carr and his coworkers make the following proposal to explain these results. Xenon is a spherical atom. When placed in a magnetic field the field at the xenon nucleus departs from the external field only because of the diamagnetic shielding produced by the Larmor circulation. As a result the field at the nucleus, H_n, is less than the applied field H_0 by an amount

$$(H_0 - H_n)/H_0 = 0.558 \times 10^{-2} \equiv \sigma \qquad (1\text{-}9)$$

More graphically, this signifies that their operating field of 8060 gauss was shielded by 45 gauss due to the circulation of the atomic electrons around the direction of the field.

If one now considers the collisions between xenon atoms it is clear that during the time of collision, τ_c, this circulation will be somewhat interupted; σ will decrease by an amount $\delta\sigma$ to some smaller value only to return to its original value after the collision is over. Since τ_c as well as the time τ *between* collisions are small compared to the period of the nuclear precession, the nucleus will see only the time average of the fluctuating diamagnetic shielding field. If σ' is the shielding constant in the presence of collisions, and if $(\tau_c/\tau) << 1$, it follows that

$$\sigma' - \sigma \cong \langle \delta\sigma(\tau_c/\tau) \rangle \qquad (1\text{-}10)$$

where the average is taken over the energy distribution in the gas. If one crudely regards $\delta\sigma$ and τ_c as independent of the kinetic energy of the atoms and uses a hard sphere model for the collisions between atoms, then

$$\langle 1/\tau \rangle = 4a^2\rho(\pi kT/m)^{1/2} \qquad (1\text{-}11)$$

where a is the diameter of the atom, m is the mass of the atom, and ρ is the number of atoms/cc. Thus

$$\delta H_0/H_0 = \sigma' - \sigma = \delta\sigma\tau_c\, 4a^2(\pi kT/m)^{1/2}\rho \qquad (1\text{-}12)$$

The result in equation 1-12 suggests that it would be most interesting to study the temperature-dependence of $\delta H_0/H_0\rho$.

While the treatment above is admittedly crude, it seems clear that further experiments along the lines begun by Carr will throw light on the details of atomic collisions and on the alteration in the diamagnetic shielding during such collisions.

2. Relaxation and Diffusion in Liquids and Gases

2.1 Liquids: The Hydrocarbons and Water

The first nuclear resonance experiment performed under high pressure was a study of the nuclear relaxation times and molecular self diffusion constants of liquids. The experiment was proposed by E. M. Purcell and carried out by the author as his Ph.D. thesis (18,19). Measurements were made of the nuclear spin-lattice relaxation times, T_1, of the proton in the liquids *n*-pentane, *n*-hexane, toluene, ethyl iodide, methyl iodide, and water, at room temperature and in the pressure range 1 to 10,000 kg/cm.^{2} Also, the effect of pressure on the self diffusion constant, D, of methyl iodide and water was determined. Both T_1 and D were measured using the spin echo techniques discovered by E. L. Hahn (21,20).

The physical ideas which underly this study are as follows: As was mentioned previously in Chapter I, Section 3.1, the nuclear spin-lattice relaxation time T_1 is the time required for the nuclear moments to establish a Boltzmann distribution among the nuclear Zeeman levels produced by the application of a magnetic field, H_0. The equilibrium difference in population between these levels results from transitions produced by fluctuating fields at the nucleus. In the case of protons in diamagnetic liquids the fluctuating field at a given nucleus is produced by the magnetic dipole moment of nuclei within the molecule as well as those in other surrounding molecules. Bloembergen, Purcell, and Pound (22) have presented the theory

of nuclear relaxation. Their theory in the particular case of the water molecule gives the following expression* for T_1

$$\frac{1}{T_1} = \left(\frac{3}{2}\frac{\gamma^4\hbar^2}{b^6}\tau_c + \frac{\pi}{5}\frac{\gamma^4\hbar^2}{a}\frac{N_0}{D}\right) \tag{2-1}$$

where

- γ is the nuclear gyromagnetic ratio of the proton
- b is the interproton distance in the water molecule
- τ_c is the correlation time for molecular reorientation. It is a measure of the time during which a molecule maintains a particular spatial orientation
- N_0 is the number of molecules/cc
- a is the molecular radius of the water molecule
- D is the selfdiffusion constant for water

It has been assumed in writing equation (2-1) that $\tau_c << 1/\omega_0$, where $\omega_0/2\pi$ is the nuclear Larmor frequency. This assumption is valid throughout the pressure range employed. The first term in equation (2-1) is the contribution to T_1 from the magnetic dipole-dipole interaction between the two protons within the H_2O molecule. Random reorientations of the molecule modulate this interaction by changing the angle between the nuclear spin vectors and the line joining the two nuclei. τ_c characterizes the time for molecular reorientation. The second term in equation (2-1) comes from the fluctuating fields produced by the diffusional motion of nuclear magnetic dipoles in molecules surrounding the molecule in question. Equation (2-1) can be generalized to apply to more complicated molecules, the only alteration being changes in the coefficients of τ_c and N_0/D.

In order to make contact with the macroscopic properties of the liquid it is necessary to relate τ_c to some macroscopic parameter. Bloembergen, Purcell, and Pound did this by noting

* The expression for T_1 given in Reference 22 contains a numerical error. This is corrected in the treatise of A. Abragam (Reference #27, pp. 300–302), whose results we quote.

that the time required for a translational diffusion jump is connected to the diffusion coefficient D by

$$\tau_D = 2a^2/9D \tag{2-2}$$

By further assuming that the correlation time τ_c for reorientation is proportional to that for translation, they could relate τ_c to D. This proportionality assumption is

$$\tau_c = \Lambda\tau_D \tag{2-3}$$

where Λ is regarded as a numerical constant of the order of unity. Under this assumption equation (2-1) becomes

$$1/T_1 = [(\gamma^4\hbar^2a^2\Lambda/3b^6) + (\pi/5)(\gamma^4\hbar^2N_0/a)](1/D) \tag{2-4}$$

The final step in the transition to macroscopic quantities is to make use of the Stokes-Einstein relation, which connects the viscosity η to D and the temperature T by

$$D = kT/8\pi\eta a \tag{2-5}$$

where k is Boltzmann's constant. Thus T_1 can be written in terms of the viscosity as

$$1/T_1 = 8\pi\gamma^4\hbar^2[(a^3\Lambda/3b^6) + N_0(\pi/5)](\eta/kT) \tag{2-6}$$

for the H_2O molecule. For molecules containing more than two protons, equation (2-6) can be generalized to

$$1/T_1 = (\alpha\Lambda + \beta N_0)(\eta/kT) \tag{2-7}$$

Thus, according to this theory T_1 should vary inversly as the viscosity η. Measurements that changed η by changing the temperature did in fact confirm the validity of equation (2-7). However, it is by no means obvious that the transition from the microscopic equation (2-1) to the macroscopic (2-6) will be valid when τ_c and D are altered by changing the pressure. Bridgman had already measured (23) the effect of pressure on the viscosity of a number of liquids, and had shown that η increases by a factor of 10 or 100 on increasing the pressure to 10,000 kg/cm^2. With this information already available it

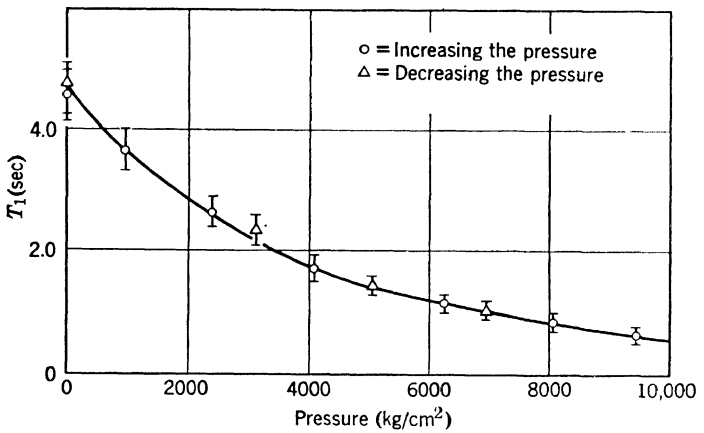

Figure 12. The pressure-dependence of the relaxation time, T_1, for the protons in *n*-pentane at 27° C.

seemed appropriate to measure T_1 vs. pressure to examine the validity of equation (2-1).

In order to carry out the experiment it was first necessary to develop a nonmagnetic pressure chamber with an electrical plug capable of transmission of radio-frequency power into the high-pressure region. Following a suggestion by Bridgman, beryllium-copper was used as the material for the pressure vessel. It proved successful from the start and has been a basic ingredient of magnetic resonance experiments at high pressure ever since. An electrical plug constructed of the same material was also designed (18,19) and found quite satisfactory.

Typical results for T_1 vs. pressure may be seen in Figure 12, which gives the data on *n*-pentane, $CH_3(CH_2)_2CH_3$, from 1 to 10,000 kg/cm^2 at room temperature. The relaxation time decreases by about a factor of 9 to 10,000 atmospheres. However, as is shown in Figure 13, which plots $(1/\eta(P)/(1/\eta(0))$ as well as $(T_1(P)/T_1(0))$ on a semilog plot, the viscosity increases by a factor of 40. The data of Figure 13 show conclusively that T_1 is not proportional simply to $1/\eta$, but that the product $T_1\eta$

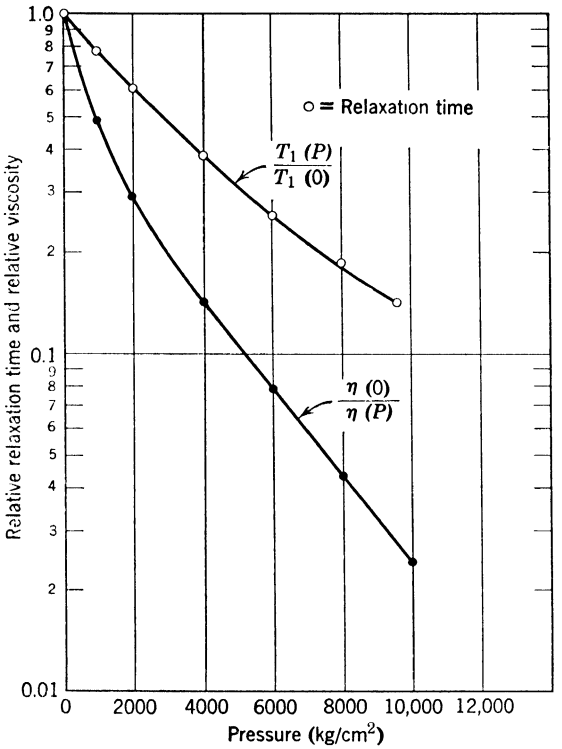

Figure 13. The pressure-dependence of the normalized relaxation time $T_1(P)/T_1(0)$ and the reciprocal of the normalized viscosity $\eta(0)/\eta(P)$ for pentane at 27° C.

increases as the pressure rises. In the case of *n*-pentane, $T_1\eta$ increases by a factor of 4 or 5 in 10,000 kg/cm.^{2} Similar results were found for all the other liquids.

In searching for the reason for the breakdown of equations (2-6) and (2-7), one must consider the possibility that the Stokes-Einstein relation (equation (2-5)) does not hold. To examine this possibility, the spin echo method (21) was used to measure the diffusion constant directly. It was convenient to do

this for water, for which η is known as a function of pressure. This measurement showed (19) that D was indeed proportional to $(1/\eta)$ over the entire pressure range. However T_1 was not proportional to $(1/\eta)$. Furthermore D was also measured under pressure for methyl iodide. Viscosity data were not available for this liquid, but comparisons with T_1 as a function of pressure showed that T_1 decreased more slowly than did D as the pressure increased. This indicates that equation (2-4), which does not use the Stokes-Einstein relation, also fails.

The difficulty therefore appears to lie not in the Stokes-Einstein relation, but rather in the assumption that τ_c is strictly proportional to τ_D, as given in equation (2-3). The experimental results in fact imply that Λ decreases markedly on increasing the pressure. For example, in *n*-pentane it must decrease by a factor of 5 or more on increase to 10,000 kg/cm^2. This implies that a reduction of the free volume of the liquid increases τ_D much more than τ_c. This result is in fact quite reasonable, and may be understood in the following way: We may relate τ_c and τ_D to activation energies for reorientation and translation by $\tau_c \propto \exp(\Delta E_r/kT)$ and $\tau_D \propto \exp(\Delta E_t/kT)$, where ΔE_r and ΔE_t represent the barrier against reorientation and translation respectively. At atmospheric pressure, the constancy of Λ on changing the temperature implies $\Delta E_r = \Delta E_t$. However, on reducing the free volume of the liquid it is entirely reasonable to expect that the barrier against translation (ΔE_t) will increase more than that against rotation (ΔE_r). In a classical picture, the barrier against rotation for a spherical molecule will be independent of the pressure, while that against translation will clearly increase. In such circumstances $\Lambda = \exp(\Delta E_r - \Delta E_t)/kT$ can be expected to decrease markedly, as is consistent with the experimental observations.

In summary, it may be said that this experiment helped to clarify a delicate point in the theory of nuclear relaxation in liquids; in so doing it threw light on the details of molecular motion in liquids. Its final, and perhaps most important, result was to show that not only magnetic resonance experiments, but

other experiments (24) requiring magnetic fields can be performed at high pressure.

A possible source of objection to this experiment was later investigated by A. W. Nolle and P. P. Mahendroo (25). These workers carefully removed from the liquids dissolved paramagnetic impurities, the most important of which is oxygen, by pumping on them, and by adding magnesium filings. The range of pressure in these experiments was from 1 to 1400 atmospheres. Comparison of their results in this narrow pressure range with those discussed above showed that while T_1 decreased somewhat more with pressure than did the unpurified material, it still did not decrease nearly as much as the reciprocal of the viscosity.

Following the measurement of the pressure-dependence of the diffusion constants of water and methyl iodide (19) by the spin echo method, D. McCall, D. C. Douglass, and E. Anderson (26), using the same techniques, made an extensive study of the temperature- and pressure-dependence of D in *n*-pentane, *n*-hexane, *n*-heptane, *n*-octane, *n*-nonane, *n*-decane, 2-methylpentane, 3-methylpentane, 2,2-dimethylbutane and 2,3-dimethylbutane. While their beryllium-copper bomb was capable of pressures up to about 7,000 atmospheres, the experimental range actually employed was only about 600 atmospheres. From their measurements of D vs. temperature at atmospheric pressure they determined the activation energy for selfdiffusion at constant volume (E_V). This quantity is given by

$$E_V = -R(\partial \ln D/\partial(1/T))_V \tag{2-8}$$

(See also Chapter I, Section 3.1). From the pressure measurements they found the pressure derivative of the activation energy, i.e., the activation volume, ΔV_a. This quantity is given by

$$\Delta V_a = -RT(\partial \ln D/\partial P)_T \tag{2-9}$$

Comparison of the activation volume with the molar volume V shows that the ratio $\Delta V_a/V$ is between 10% and 14% for almost

all the liquids studied. This ratio rises to 20% only in the case of 2,2-dimethylbutane. These workers also made the empirical observation that $\Delta V_a/V$ was equal, within experimental error, to the ratio of the activation energy at constant volume to the heat of vaporization E_{vap}, i.e.

$$\Delta V_a/V \approx E_V/E_{\text{vap}} \tag{2-10}$$

2.2 Gases: Hydrogen, Methane, Ethylene, and Xenon

The theory of nuclear relaxation in hydrogen was first given in the classic paper of Bloembergen, Purcell, and Pound (22,27). As has been emphasized before (Chapter I, Section 3-3), hydrogen gas may be regarded as a mixture of two distinct molecules: ortho and parahydrogen. The ortho molecules have $I = 1$, and may have the rotational quantum numbers $J = 1,3,5 \ldots$, while the para molecules have $I = 0$ and may have $J = 0,2,4 \ldots$ Only the ortho molecules contribute to the nuclear resonance, and since the difference in energy between the $J = 1$ and $J = 3$ states is about 850° K these molecules are largely in the $J = 1$ state provided that the temperature is not too high. The statistical degeneracy of the $J = 1$ state is 3, while that of the $J = 0$ state is 1, so that normal hydrogen is in fact a mixture of 25% para molecules and 75% ortho molecules.

In the free hydrogen molecule, the magnetic fields seen by the nuclei come primarily from the magnetic dipole-dipole interaction between protons

$$\mathcal{H}_{d-d} = \hbar\omega''[\mathbf{I}_1 \cdot \mathbf{I}_2 - 3(\mathbf{I}_1 \cdot \hat{n})(\mathbf{I}_2 \cdot \hat{n})] \tag{2-11}$$

and from the interaction between the nuclear moments and the field set up by the rotation of the molecule as a whole, i.e., the spin-rotational interaction

$$\mathcal{H}_{s-r} = \hbar\omega'(\mathbf{I}_1 + \mathbf{I}_2) \cdot \mathbf{J} \tag{2-12}$$

where J is the rotational angular momentum operator, $\mathbf{I}_1$ and $\mathbf{I}_2$ are the spin operators for the two protons, and $\hat{n}$ is a unit vector along the line joining them. There are also fields at a

given nucleus produced by surrounding molecules. This *inter*molecular contribution is negligible in the case of hydrogen both in the gaseous and liquid states.

The *intra*molecular field fluctuates as the molecule undergoes collisions which produce transition between the three rotational states ($m_J = 0 \pm 1$). This fluctuating field is responsible for the nuclear relaxation. If τ_c is the correlation time for reorientation, then as Schwinger has shown (22) the spin lattice relaxation time may be written as (27)

$$1/T_1 = [(4/3)(\omega')^2 + (3/5)(\omega'')^2]\tau_c \qquad (2\text{-}13)$$

The constants ω' and ω'' have been measured with great accuracy using molecular beams. This gives

$$\omega'/\gamma = H' = 27 \text{ gauss}$$
$$\omega''/2\gamma = H'' = 34 \text{ gauss} \qquad (2\text{-}14)$$

where γ is the gyromagnetic ratio of the proton. Using these values, we find

$$1/T_1 = (2.74 \times 10^{12})\tau_c \qquad (2\text{-}15)$$

It should be borne in mind that each collision between molecules does not produce a reorientation. Only the relatively weak anisotropic part of the intermolecular interaction can produce changes in the spatial orientation of the molecules. Thus τ_c is always longer than the mean time between collisions. From equation (2-15) we see that measurements of T_1 provide a direct determination of τ_c. It is the object of the experiments discussed below to examine the temperature- and pressure-dependence of τ_c in an effort to obtain information on the nonspherically symmetric part of the interaction between hydrogen molecules.

The relaxation time T_1 in hydrogen gas was first measured in 1946 by Purcell, Pound, and Bloembergen (28), who used a sample at a pressure of 10 atmospheres at room temperatures. It remained for M. Bloom (29,30) and M. Lipsicas to study more

extensively the pressure dependence of T_1 at various temperatures. Their pressure range was 150 atmospheres and the temperature range was $39° \text{ K} \leq T \leq 300° \text{ K}$. The dependence of T_1

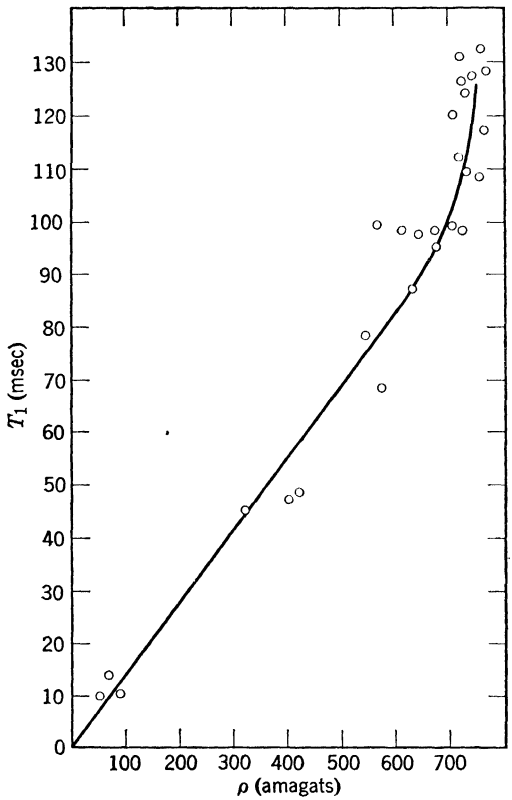

Figure 14. The relaxation time T_1 for hydrogen gas vs. the density at 37°K. Note that the amagat = (density at pressure P and temperature T)/(density at 0° C and 1 atmosphere).

on the pressure, or better yet, the density ρ, may be obtained as follows. If the density of the gas is low enough so that only binary collisions are involved, it is possible to define a cross section,

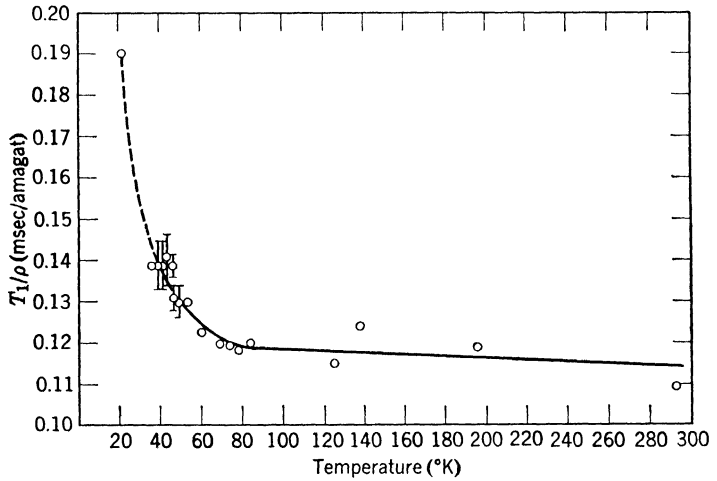

Figure 15. T_1/ρ vs. temperature for hydrogen gas.

σ_r, for the collisions producing molecular reorientation. In terms of this cross section we may write

$$1/\tau_c = \rho\langle\sigma_r v\rangle \tag{2-16}$$

where ρ is the number of molecules/cc; $\langle\sigma_r v\rangle$ is the cross section weighted by the velocity and averaged over the velocity distribution in the gas. In this formulation σ_r depends not only on the relative velocity of two molecules, but also on whether the collision is between ortho molecules or between an ortho and a para molecule. Thus σ_r as defined in equation (2-16) depends on the ortho-para ratio in the gas. In Figure 14 is shown the result of Lipsicas and Bloom for T_1 vs. ρ, where ρ is measured in units of the amagat: ρ = (density at pressure P)/(density at T = 0° C, P = 1 atmosphere). The linear region below 500 amagats gives way to a more rapid increase above 600 amagats. From the slope of T_1 vs. ρ data in the low density region they have found the temperature-dependence of $\langle\sigma_r v\rangle$ for normal hydrogen. This result is shown in Figure 15. Lipsicas and Bloom find it

difficult to explain classically the observed temperature variation of $\langle \sigma_T v \rangle$. In fact, in the region $100° \text{ K} \leq T \leq 300° \text{ K}$ they reason that σ_T should depend on velocity as $(1/v^2)$. On weighting this by v and averaging over the velocity distribution this leads to a temperature-dependence of T_1/ρ which goes as $T^{-1/2}$. This is in distinct disagreement with the observations. Furthermore, below 100° K, the kinetic energy per molecule is so low that the de Broglie wavelength becomes larger than the molecular diameter. This, they argue, should prevent the occurrence of the close encounters that are responsible for molecular reorientation. Under these conditions $\sigma_T v$ should fall as the temperature falls below 100°. The observations, on the other hand, show a marked rise in this quantity as the temperature falls.

Lipsicas and Bloom have also made a preliminary study of the dependence of (T_1/ρ) on the ortho-para concentration. This preliminary work indicates that the temperature-dependence of T_1/ρ may depend markedly on the ortho-para ratio. They also measured, by spin echo methods, the diffusion coefficient D for the ortho molecules in normal H_2 at 78° K to densities up to 500 amagats. They found that D is directly proportional to $(1/\rho)$, as is consistent with the relation (31)

$$D = f\,(\eta/m)(1/\rho) \tag{2-17}$$

where η is the viscosity of the gas, m is the mass of the molecule, and f is a numerical constant of the order of unity.

The relaxation time T_1 has also been studied as a function of pressure in methane, CH_4, and ethylene, C_2H_4 (32). These measurements for CH_4, taken at 193° K and 293 °K, give

$$\begin{aligned} T_1/\rho &= 3 \times 10^{-2} \text{ sec/amagat} \qquad \text{at } T = 193° \text{ K} \\ T_1/\rho &= 2 \times 10^{-2} \text{ sec/amagat} \qquad \text{at } T = 293° \text{ K} \end{aligned} \tag{2-18}$$

In ethylene

$$T_1/\rho = 0.25 \text{ sec/amagat} \qquad \text{at } T = 293° \text{ K} \tag{2-19}$$

An equation similar to (2-15) has been given (32) for CH_4 and C_2H_4 under the assumption that the spin-rotational interaction is small in these molecules. This assumption has been challenged by J. Waugh and C. S. Johnson (33) on the basis of recent molecular beam results. Using only the dipole-dipole field, Bloom *et al.* (32) find that

$$T_1\tau_c = 1.24 \times 10^{-11} \text{ sec}^2 \qquad \text{for } CH_4$$

and (2-20)

$$T_1\tau_c = 3.85 \times 10^{-11} \text{ sec}^2 \qquad \text{for } C_2H_4$$

From these equations and their measurements of T_1 they find the ratio τ/τ_c, where τ is the time between collisions. To estimate τ they regard the molecules as hard spheres of diameter a. The kinetic theory of gases then gives (31)

$$1/\tau = 4\, a^2\, \rho\, (\pi kT/m)^{1/2}$$

They thus estimate for CH_4 (2-21)

$$\tau/\tau_c = 0.27 \qquad \text{at } T = 193^\circ \text{ K}$$

$$\tau/\tau_c = 0.15 \qquad \text{at } T = 293^\circ \text{ K}$$

while for C_2H_4

$$\tau/\tau_c = 0.66 \qquad \text{at } T = 293^\circ \text{ K}$$

Summarizing this discussion of the experimental studies of relaxation in polyatomic gases, we observe that a theory capable of explaining the temperature-dependence of T_1/ρ for the low density region has not yet been produced. Neither has it been possible to account quantitatively for the deviations of T_1 from proportionality to ρ in the region of high density. Nevertheless it seems clear that a successful theory will throw light on the small anisotropic interactions between the molecules in the gas.

We have seen that the nuclear relaxation in polyatomic gases is produced primarily by *intra*molecular magnetic fields that fluctuate from one value to another as a result of the

collisions between molecules. The situation is quite different in a monatomic gas. In this case the relaxation is produced by the *inter*molecular fields that exist only *during* the collisions between atoms (22,27). As a result, the nuclear relaxation rate $1/T_1$ is proportional to the number of collisions per unit time. Thus if τ is the mean time between collisions, we may expect $(1/T_1)\alpha(1/\tau)$. Furthermore, since $1/\tau$ is proportional to the density ρ, we may expect in monatomic gases that the relaxation rate is proportional to the density $(1/T_1)\alpha\rho$.

Using gas pressures between 30 and 110 atmospheres, the nuclear relaxation of the xenon^{129} nucleus ($I = {}^1/_2$) has been studied (7,8) in natural xenon gas. This gas consists of 29% Xe^{129} and 21.2% Xe^{131}, which are the constituents with magnetic moments. The remaining atoms have nuclei with even mass numbers and hence no nuclear moment. These are Xe^{132}, Xe^{134}, Xe^{136}, Xe^{130}, and Xe^{128}. The nuclear signal from the Xe^{129} is weak, and the nuclear relaxation times T_1 are extremely long ($10^2 < T_1 < 3 \times 10^3$ sec), making a measurement of T_1 quite difficult. Nevertheless, E. R. Hunt and H. Y. Carr (8) have shown that when sufficient care is taken to remove paramagnetic impurities, T_1 is related to the density by

$$1/T_1 = (5.7 \times 10^{-6})\rho \qquad (2\text{-}22)$$

where ρ is measured in amagats. This dependence on the density is exactly what one would expect for relaxation through *inter*molecular fields. However, if one regards the intermolecular field as arising out of the nuclear dipole-dipole interaction, the theory gives a value for T_1 which is three orders of magnitude longer than that observed. Thus some more effective relaxation mechanisms must be operative during atomic collisions. Such a mechanism has very recently been proposed by H. C. Torrey (34).

References

1. N. F. Ramsey, *Phys. Rev.*, **78**, 699 (1950); **86**, 243 (1952).
2. A. Saika and C. P. Slichter, *J. Chem. Phys.*, **22**, 26 (1954).

3. J. Pople, W. Schneider, and H. Bernstein, *High Resolution Nuclear Magnetic Resonance*, McGraw-Hill, New York, 1959.
4. J. Roberts, *Nuclear Magnetic Resonance*, McGraw-Hill, New York, 1959.
5. J. Armstrong and G. B. Benedek, *Bull. Am. Phys. Soc.*, **6**, 233 (1961).
6. J. Armstrong, Thesis, Harvard University, 1961 (unpublished).
7. R. L. Streever and H. Y. Carr, *Phys. Rev.*, **121**, 20 (1961).
8. E. R. Hunt and H. Y. Carr, *Bull. Am. Phys. Soc.*, 7, 293 (1962).
9. W. D. Knight, *Phys. Rev.*, **76**, 1259 (1949).
10. W. C. Dickinson, *Phys. Rev.*, 77, 717 (1950).
11. R. Freeman, G. Murray, and R. Richards, *Proc. Roy. Soc.* (*London*), **A242**, 455 (1957).
12. J. S. Griffith and L. Orgel, *Trans. Faraday Soc.*, **53**, 601 (1951).
13. J. S. Griffith and L. Orgel, *J. Chem. Soc.*, *IV*, 4981 (1956).
14. S. Dharmatti and C. Kanekar, *J. Chem. Phys.*, **31**, 1436 (1959).
15. A. Abragam, J. Horowitz, and M. Pryce, *Proc. Roy. Soc.* (*London*), **A230**, 119 (1955).
16. R. L. Streever and H. Y. Carr, *Phys. Rev.*, **121**, 20 (1961).
17. E. Hunt and H. Y. Carr, *Bull. Am. Phys. Soc.*, 7, 293 (1962).
18. G. Benedek, Thesis, Harvard University, 1953.
19. G. Benedek and E. M. Purcell, *J. Chem. Phys.*, **22**, 2003 (1954).
20. E. L. Hahn, *Phys. Rev.*, **80**, 580 (1950).
21. H. Y. Carr and E. M. Purcell, *Phys. Rev.*, **94**, 630 (1954).
22. N. Bloembergen, E. M. Purcell, and R. V. Pound, *Phys. Rev.*, **73**, 679 (1948).
23. P. W. Bridgman, *The Physics of High Pressures*, G. Bell and Sons, Ltd., London, 1949.
24. G. B. Benedek, W. Paul, and H. Brooks, *Phys. Rev.*, **100**, 1129 (1956).
25. A. W. Nolle and P. P. Mahendroo, *Bull. Am. Phys. Soc.*, **4**, 166 (1959).
26. D. W. McCall, D. C. Douglass, and E. W. Anderson, *Phys. Fluids*, **2**, 87 (1959).
27. A. Abragam, *Principles of Nuclear Magnetism*, Oxford University Press, 1961.
28. E. M. Purcell, R. V. Pound, and N. Bloembergen, *Phys. Rev.*, **70**, 986 (1946).
29. M. Bloom, *Proc. Intern. Conf. Low. Temp. Phys., 7th, Toronto, Ont.*, 4-1 (1961).
30. M. Lipsicas and M. Bloom, *Can. J. Phys.*, **39**, 881 (1961).
31. J. Hirschfelder, C. Curtis, and R. Bird, *Molecular Theory of Gases and Liquids*, John Wiley and Sons, New York, 1954.
32. M. Bloom, M. Lipsicas, and B. H. Muller, *Can. J. Phys.*, **39**, 1093 (1961).
33. J. Waugh and C. S. Johnson, *J. Chem. Phys*,. **36**, 2266 (1962).
34. H. C. Torrey, *Phys. Rev.*, **130**, 2306 (1963).

Experimental Methods

The methods and materials required to carry out magnetic resonance experiments in the pressure range from 1 to 65 kilobars and the temperature region from 1° K to 400° K are necessarily quite varied. Nevertheless, we may roughly divide these methods and materials into the following categories: (*a*) pressure-transmitting media, (*b*) pressure multipliers, (*c*) pressure vessels for the samples and electrical plugs, and (*d*) pressure-measurement methods.

A liquid pressure-transmitting medium which has a very wide useful temperature and pressure range is a 50-50 mixture of *n*-pentane and 2-methylbutane. Bridgman used this mixture in his experiments to 30 kilobars at room temperature. It can also be used (1) to transmit pressure to at least 10 kilobars without freezing at 196° K. Petroleum ether is a liquid very commonly used at room temperature in the region of 12 kilobars. Fuke has shown (2) that this liquid does not freeze at 90° K provided that the pressure is below 1000 bars. His observation suggests that it may be possible to find other liquids which do not solidify at 77° K, provided that the pressure is kept rather low, say, below 5 kilobars. Normally though, below 77° K helium gas is used as the hydrostatic pressure-transmitting medium. The melting curve of helium below 40° K has been obtained by Mills and Grilly (3) and between 35° K and 50° K by Holland, Huggill, and Jones (4). In Table A-1 the freezing pressure, P_F, of helium is listed as a function of temperature, T. The Simon melting equation applies rather well to the data, so that

TABLE A-1

T (° K)	1	4.2	10	20	30	40	50
P_f (atm)	25	140	580	1700	3300	5100	7300

for extrapolation above 50° K one may employ the relation (4)

$$(P_F/16.45) = (T/0.992)^{1.554} - 1$$

where P_F is measured in atmospheres, T in ° K. If it is necessary to conduct experiments at higher pressures than the freezing pressure of helium it is possible to use solid hydrogen or solid helium. The work of Dugdale and Hulbert (5) is very encouraging as to the hydrostatic nature of the stress transmitted by the highly-compressible solid helium. Similarly, Jennings and Swenson (6) have found that solid hydrogen may be used satisfactorily as a transmitter of approximately hydrostatic pressure up to 10 kilobars through their experiments on the effect of pressure on the superconducting transition temperature of a number of metals. In order to carry out magnetic resonance experiments into the 100 kilobar region AgCl can be used as a pressure-transmitting medium. This material apparently is capable of transmitting the pressure hydrostatically to a powder sample intimately dispersed in the AgCl. The sample geometry used in a magnetic resonance experiment to 65 kilobars will be described in a succeeding paragraph (see Figure A-4).

The compression of the transmitting medium is produced by a pressure multiplier or high-pressure press. Such a press essentially consists of two pistons connected to one another. One piston has a large area, A_1, the other has a small area, A_2. A low-pressure hydraulic pump applies a pressure P_1 to the large piston. This in turn pushes on the smaller piston. The pressure P_2 at the end of the narrow piston is therefore given by $P_2 = P_1(A_1/A_2)$, i.e., the pressure generated by the low-pressure pump is multiplied by (A_1/A_2). The design considerations connected with these multipliers can be found in a number

of books and review articles (7,8,9,10). Presses suitable for gaseous or liquid transmitting media are readily available from a number of commercial firms. The pressures developed in such presses may be conveyed very conveniently to the vessel containing the sample by the use of hard-drawn Type 316 stainless steel tubing (11), o.d. $^1/_8$″, i.d. 0.025″. Warschauer and Paul (11) have found that this tubing, which is flexible and has a low thermal conductivity, can withstand an internal pressure near 20,000 atmospheres before bursting. Presses suitable for use with solid hydrogen or helium as pressure-transmitting media have been described by Swenson (6,12) and Stewart (13). The superpresses for operation up to the 100 kilobar region are commercially available in the form of "belts" (14), "tetrahedra," and piston and cylinder combinations.

Magnetic resonance experiments normally require the application of a magnetic field. Hence, nonmagnetic pressure vessels to contain the sample are usually necessary. It has been found (15) that beryllium-copper, a precepitation-hardening alloy of 98% Cu and 2% Be (by weight) may be used successfully for this purpose. The specific alloy generally employed is solution-annealed Berylco No. 25, which is easily machined. However beryllium powder is toxic, so that adequate ventilation should be provided if grinding operations are performed. Normal machining under oil should cause no difficulties. After machining, the material may be hardened by heating at 325° C for 3 hours and then quenching in oil. This should bring the hardness up to Rockwell C-39 to C-41. Beryllium-copper pressure vessels have proven themselves at room temperatures to 20,000 atmospheres (16), and at or below 4° K to 10,000 atmospheres. An article reviewing experience in fabricating Be-Cu pressure vessels has been published (16).

Of these experiences, one hard-won lesson is particularly worth mentioning. The normally available Be-Cu rod or bar stock, instead of being homogeneous in the interior, occasionally contains bubbles of gas. This imperfection is known as "pipe" or "porosity." If such material is employed in the construction

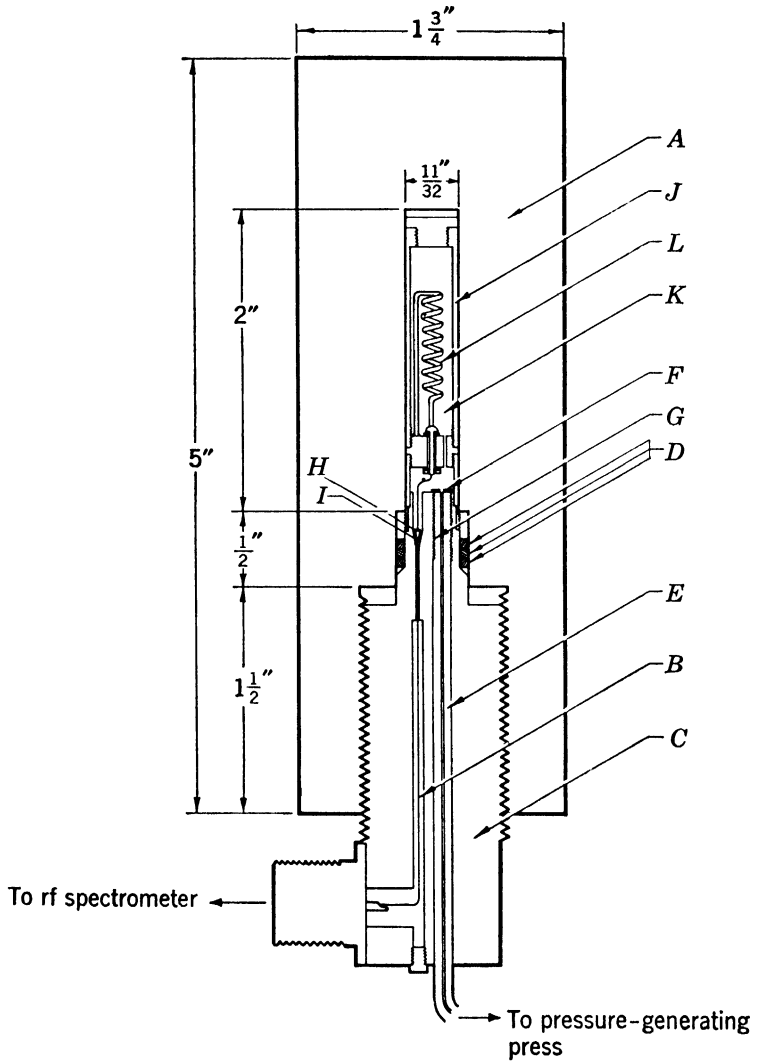

Figure A-1. Beryllium-copper pressure vessel and electrical plug used with a liquid pressure-transmitting medium for nuclear resonance experiments to 10,000 bars.

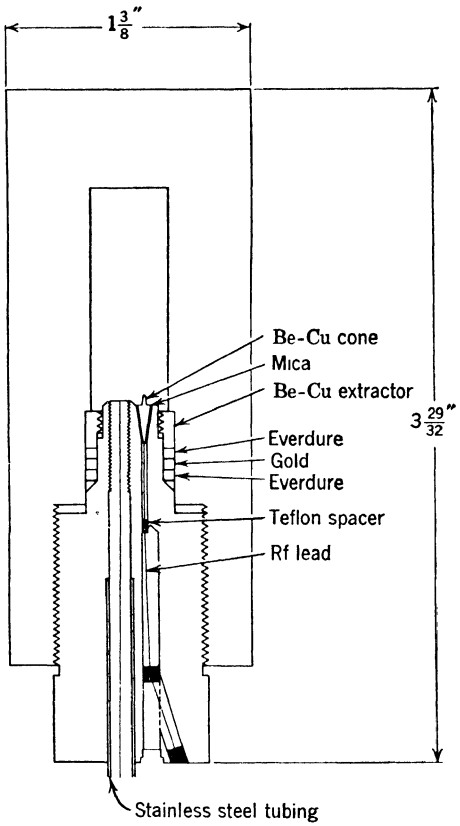

Figure A-2. Small pressure vessel and electrical plug used for nuclear resonance experiments with helium as the pressure-transmitting medium below 77° K.

of a pressure vessel, the gas bubbles act as stress risers and the bomb will crack under pressure. Ultrasonic testing before fabrication is often helpful in detecting such flaws. Nevertheless, initial tests of a new bomb under pressure should be made with adequate protective shielding. Stainless steel has also been used as material for pressure vessels (16). It should be

kept in mind that in the case of pure quadrupole resonance or nuclear resonance in ferromagnets, antiferromagnets, and ferrimagnets, an external magnetic field is not necessary. In such experiments steel may be used for the pressure vessel.

In order to bring electrical leads into the high-pressure region it has proved possible to adapt the conical seal of Bridgman for use in the radio-frequency and microwave region. In the previous figures below we see examples of pressure vessels and electrical plugs used in various frequency regions. Figure A-1 shows a typical beryllium-copper high-pressure vessel (*A*) and electrical plug (*C*) used in nuclear magnetic resonance experiments (1) to 10,000 atmospheres with liquid pressure transmitters. The rf current passes into the high-pressure region along small-diameter wire (*B*) which connects to the cone (*H*). This cone seals against leak by pressing against a conical insulator (*I*) of artificial mica or lava. These conical seals have been used successfully from d.c. through 200 mc (2). A flexible connection makes contact from the cone to the rf coil (*L*) inside the sample holder (*J*). The pressure transmitting liquid passes into the vessel through the stainless steel tubing (*E*) which is snugly threaded and sweat soldered into the plug at *G*. A soft copper plate may be soldered over the end of this connection to prevent the high-pressure liquid from forcing its way into and ultimately past the threads (*G*). The entire plug is sealed in the bomb with Bridgman's arrangement of packing washers (*D*). The center washer is lead while the other two are Everdure. It is worth noticing that this 10,000 atmosphere system is quite small. Its o.d. is only $1^3/_4''$ and its length is about $5^1/_2''$ overall. It is used very conveniently with high- or low-temperature baths inserted within the pole faces of an electromagnet. A smaller beryllium-copper system used for operation (17) at temperatures below 70° K and for pressures below ~2500 atmospheres is shown in Figure A-2. To assist in sealing the cones at low temperatures against leakage of the gaseous pressure-transmitting medium (usually helium) it is helpful to smear some Dow-Corning silicon fluid No. 200 (viscosity: 12,500

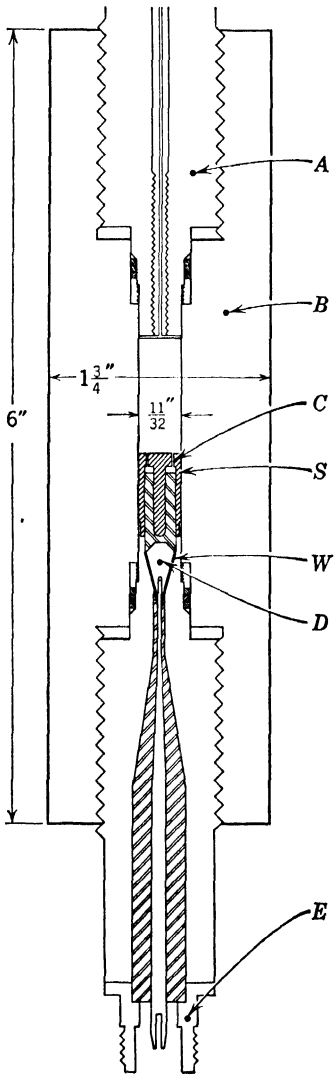

Figure A-3. Pressure vessel and microwave plug used to 10,000 bars.

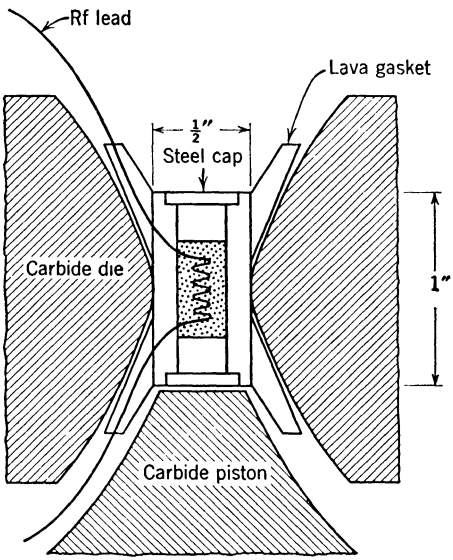

Figure A-4. Radio-frequency coil and sample assembly at the center of a belt-type press for a magnetic resonance experiment to 65,000 bars.

centistokes) over the end of the cones. Also, in this system the central washer of the three sealing the plug should be gold rather than lead. The thermal contraction of gold is less than that of Be-Cu, thus a seal made at room temperature will maintain itself at low temperature.

In Figure A-3 we show the microwave high-pressure system of Walsh and Bloembergen (18) which operates to 10,000 atmospheres. The system has two separate beryllium-copper plugs. The upper plug (*A*) is used to introduce the pressure fluid, while the lower is the microwave transmission plug which is designed to operate around 9 kmc. The microwave connection starts at a standard 50-ohm transmission line which tapers to 0.100″ o.d. At the conical Be-Cu plug (*D*) the line tapers out to 0.250″ o.d. The cone seats on an artificial mica washer (*W*) which serves as insulator and pressure seal. The

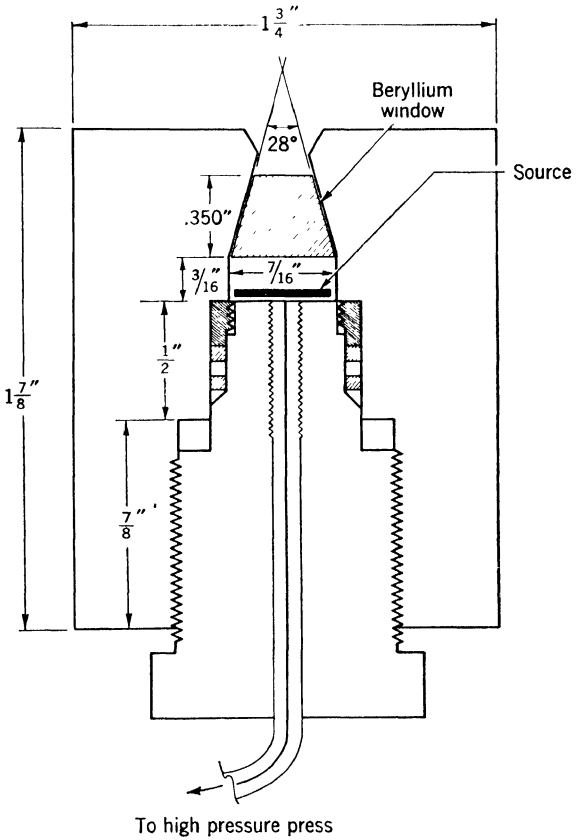

Figure A-5. Small pressure vessel with beryllium window used in a γ-ray resonant absorption experiment.

microwave cavity is press fitted on the end of this transmission line. The cavity (C) is coaxial with center stub $\lambda/4$ long (T.E.M. mode). The coupling to the transmission line is capacitive and is adjusted by changing the gap between the center stub and the cone. The sample is placed at the upper end of the cavity where the microwave magnetic field is maximum and the electrical

field is minimum. The remaining volume of the cavity is filled with Teflon or polystyrene. The loaded Q of this cavity is about 500. For operation at higher frequencies it is possible to couple into the microwave cavity through a sapphire window. This method has been developed by Lawson and Smith (19) for use around 24 kmc. Since sapphire is transparent, their design may be used for optical as well as microwave experiments to 10,000 atmospheres.

In Figure A-4 we show the central portion of a belt-type press (14) within which one can generate pressure up to the 100 kilobar region. This type press has been used (20) to conduct nuclear resonance experiments at 45 mc in ferromagnetic iron to 65 kilobars. The sample is powdered iron which is dispersed in low concentration in a matrix of AgCl. The rf coil passes out of the lava cylinder surrounding the sample, and through holes in the conical sealing gaskets.

Figure A-5 shows a small beryllium-copper bomb with a beryllium window. This vessel was used to study the effect of pressure on the energy of the γ-ray emitted from the excited state of the Fe^{57} nucleus in iron (21). The beryllium window will permit transmission of x-rays or γ-rays at least up to 3500 atmospheres. A test of this system to 10,000 atmospheres failed due to extrusion of the beryllium out the conical hole at about 9500 atmospheres. This failure may have been caused by the fact that the beryllium was originally fabricated by extrusion through dies along the same direction as that of the cone axis. A different orientation of the cone relative to the original extension axis may correct this difficulty.

The measurement of the pressure transmitted by liquid or gaseous media has been greatly facilitated by Bridgman's observation (7) that the resistance of manganin wire varies linearly with pressure at least to 13,000 atmospheres. By calibrating a coil of manganin wire at one fixed pressure point and at atmospheric pressure the variation of coil resistance with pressure can be established and the coil used as a pressure gauge. The point most frequently to calibrate the manganin

gauge coils is the freezing pressure of mercury at 0° C. This pressure (P_M) has been evaluated very precisely recently by D. H. Newhall, L. H. Abbot, and R. A. Dunn (22) using a very accurate controlled-clearance piston gauge (23) (sometimes called a dead-weight piston gauge). These workers find P_M = 7566.2 ± 3.8 (bars) or 7715.6 ± 3.8 (kg/cm^2). This result is about 1% larger than Bridgman's 1911 determination of P_M = 7640 (kg/cm^2).

For measurements of pressure in the ultrahigh pressure region where solid pressure-transmitting media are employed, the following fixed transition points have been established (24): bismuth I-II, 25,410 ± 95 bars; thallium I-III, 36,690 ± 100 bars; barium II-III, 58,600–59,100 kilobars (25). These transitions may be detected by the change in the electrical resistance of wires made of these elements.

References

1. T. Kushida, G. Benedek, and N. Bloembergen, *Phys. Rev.*, **104,** 1364 (1956).
3. T. Fuke, *J. Phys. Soc. Japan*, **16,** 266 (1961).
3. R. L. Mills and E. R. Grilly, *Phys. Rev.*, **99,** 480 (1955).
4. F. A. Holland, J. Huggill, and G. O. Jones, *Proc. Roy. Soc.* (*London*), **A207,** 268 (1951).
5. J. S. Dugdale and J. A. Hulbert, *Can. J. Phys.*, **35,** 720 (1957).
6. L. D. Jennings and C. A. Swenson, *Phys. Rev.*, **112,** 31 (1958).
7. P. W. Bridgman, *The Physics of High Pressure*, G. Bell and Sons, Ltd., London, 1949.
8. *Solids Under Pressure*, Chapter 15, Ed. W. Paul and D. Warschauer, McGraw-Hill, New York, 1963.
9. *Ind. Eng. Chem.*, **48,** 826 (1956); **49,** 1945 (1957).
10. C. A. Swenson, "Physics at High Pressure," *Advances in Solid State Physics*, Vol. 11, Ed. Seitz and Turnbull, Academic Press, New York, 1960.
11. D. M. Warschauer and W. Paul, *Rev. Sci. Instr.*, **29,** 675 (1958).
12. C. A. Swenson and R. H. Stahl, *Rev. Sci. Instr.*, **25,** 608 (1954).
13. J. W. Stewart, *Phys. Chem. Solids*, **1,** 146 (1956).
14. H. T. Hall, *Rev. Sci. Instr.*, **31,** 125 (1960).
15. G. B. Benedek and E. M. Purcell, *J. Chem. Phys.*, **22,** 2003 (1954).

16. W. Paul, G. B. Benedek, and D. M. Warschauer, *Rev. Sci. Instr.*, **30,** 874 (1959).
17. P. Heller and G. B. Benedek, *Phys. Rev. Letters*, **8,** 428 (1962).
18. W. M. Walsh and N. Bloembergen, *Phys. Rev.*, **107,** 904 (1957).
19. A. Lawson and G. E. Smith, *Rev. Sci. Instr.*, **30,** 989 (1959).
20. J. D. Litster and G. B. Benedek, *J. Appl. Phys.*, **34,** 688 (1963).
21. R. V. Pound, G. B. Benedek, and R. Drever, *Phys. Rev. Letters*, **7,** 405 (1961).
22. D. H. Newhall, L. H. Abbot, and R. A. Dunn, Annual Meeting ASME, Nov. 1962, Paper No. 62-WA-283.
23. D. P. Johnson and D. H. Newhall, *Trans. ASME*, **75,** 301 (1953).
24. G. C. Kennedy and P. N. LaMori, *Progress in Very High Pressure Research*, Ed. Bundy, Hibbard, and Strong, John Wiley and Sons, New York, 1961, p. 304.
25. G. C. Kennedy, private communication, 1962.

Index